

UCRL-10755

**University of California**  
**Ernest O. Lawrence**  
**Radiation Laboratory**

TWO-WEEK LOAN COPY

*This is a Library Circulating Copy  
which may be borrowed for two weeks.  
For a personal retention copy, call  
Tech. Info. Division, Ext. 5545*

**THE INFLUENCE OF TENSILE STRESS ON GASEOUS  
PERMEATION IN GLASSY-STATE AND  
COMPLEX CERAMICS**

**Berkeley, California**

## **DISCLAIMER**

This document was prepared as an account of work sponsored by the United States Government. While this document is believed to contain correct information, neither the United States Government nor any agency thereof, nor the Regents of the University of California, nor any of their employees, makes any warranty, express or implied, or assumes any legal responsibility for the accuracy, completeness, or usefulness of any information, apparatus, product, or process disclosed, or represents that its use would not infringe privately owned rights. Reference herein to any specific commercial product, process, or service by its trade name, trademark, manufacturer, or otherwise, does not necessarily constitute or imply its endorsement, recommendation, or favoring by the United States Government or any agency thereof, or the Regents of the University of California. The views and opinions of authors expressed herein do not necessarily state or reflect those of the United States Government or any agency thereof or the Regents of the University of California.

Research and Development

UCRL-10755  
UC-25 Metals,  
Ceramics and  
Materials  
TID-4500 (19th Ed.)

UNIVERSITY OF CALIFORNIA

Lawrence Radiation Laboratory  
Berkeley, California

Contract No. W-7405-eng-48

THE INFLUENCE OF TENSILE STRESS ON GASEOUS  
PERMEATION IN GLASSY-STATE AND COMPLEX CERAMICS

Orlin M. Stansfield

(M. S. Thesis)

April 2, 1963

Printed in USA. Price \$1.50. Available from the  
Office of Technical Services  
U. S. Department of Commerce  
Washington 25, D.C.

THE INFLUENCE ON TENSILE STRESS ON GASEOUS  
PERMEATION IN GLASSY-STATE AND COMPLEX CERAMICS

Contents

Abstract . . . . .	v
I. Introduction . . . . .	1
A. Mathematics of Gaseous Permeation through Complex Ceramics . . . . .	2
1. Volume Diffusion . . . . .	2
2. Volume Diffusion in a Stressed System. . . . .	5
3. Stress-Induced Knudsen Flow . . . . .	8
B. Earlier Experimental Investigations . . . . .	8
II. Experimental Procedure . . . . .	10
A. Specimens . . . . .	11
1. Composition and Physical Properties . . . . .	11
2. Specimen Preparation . . . . .	11
3. Microstructure . . . . .	15
B. Apparatus . . . . .	21
1. Loading Arrangement . . . . .	21
2. Cycling Arrangement . . . . .	24
3. Furnace Arrangement . . . . .	24
4. Temperature Arrangement. . . . .	27
5. Power Supply . . . . .	27
6. Atmosphere Control . . . . .	27
7. Flow-Rate Measurement . . . . .	27
8. Calibration of Equipment . . . . .	29
C. Test Procedure . . . . .	30
1. Modified Specimens . . . . .	30
2. Unmodified Specimens . . . . .	32

III. Experimental Results	
A. Alumina 1 and 2 . . . . .	33
B. Mullite 1. . . . .	33
C. Mullite 2. . . . .	42
D. Fused Silica. . . . .	43
E. Loading-Rate Dependence . . . . .	46
IV. Discussion	
A. Alumina 1 and 2 . . . . .	47
B. Measurement of K and D in Mullite 1 . . . . .	47
C. Glassy-Phase Composition of Mullite 1 . . . . .	48
D. Effect of Crystalline Content on Gaseous Permeation . . . . .	49
E. Stress Dependence of Permeation in Mullite and Fused Silica . . . . .	50
V. Summary and Conclusion . . . . .	52
Acknowledgments . . . . .	53
Appendices	
A. Calibration of the Loading Device (Diaphragm Cylinder) . . . . .	54
B. Calibration of the Helium Leak Detector . . . . .	56
C. Mathematics of the Method of Determination of Diffusion and Permeation Coefficients . . . . .	57
D. <u>Experimental Data Tables</u> . . . . .	63
References . . . . .	70

THE INFLUENCE OF TENSILE STRESS ON GASEOUS  
PERMEATION OF GLASSY-STATE AND COMPLEX CERAMICS

Orlin M., Stansfield  
Lawrence Radiation Laboratory  
University of California  
Berkeley, California

April 2, 1963

ABSTRACT

The influence of static and dynamic uniaxial tensile stress on the steady-state permeation of helium through multiphase, polycrystalline ceramics and fused silica was investigated. Tests on alumina, mullite, and pure fused silica were conducted at temperatures between 25 and 1000°C and at tensile stress levels of 0 to 12 000 psi. A mass spectrometer was used to detect helium permeation.

No permeation through alumina was detected. Gaseous permeation through mullite specimens of two different microstructures and fused silica specimens was detected and appeared to be an activated process. An increase in the gaseous permeation rate on the order of 1% upon application of a tensile stress of 4000 to 5000 psi was found, and was apparently due to a decrease in the activation energy of helium diffusion through the glassy phase. The introduction of gas-conducting channels, such as cracks and separated phase boundaries, through induced tensile stress was not detected.

The temperature dependence of Young's modulus of the glassy phase influenced the measured stress effect: a decrease in the modulus at high temperatures enhanced the effect of stress on permeation rate. Closed pores and crystalline phases seemed to influence the absolute magnitude of the stressed and unstressed permeation rate.

## I. INTRODUCTION

The term "complex ceramic", as used in this work, means a polycrystalline multiphase ceramic which may include void volume.

Very high-purity (> 99%) sintered oxide ceramics are usually permeable to gases. Control of the ceramic composition may result in the formation of a glassy phase that fills gas-conducting channels to give an impermeable body. Therefore, ceramics used to contain or exclude gases normally contain a glassy phase and are complex.

Complex ceramics, because they have brittle fracture, show a wide range of mechanical strength. One possible contribution to brittle fracture may be the existence of random weak-phase boundaries, or other non-stress-bearing surfaces within the ceramic.

If these flaws exist, it is possible that they may not permit gaseous permeation in the unstrained condition, but when distorted by strain will conduct gas in detectable amounts.

Recent development in nuclear technology has included the use of refractory ceramic materials as fuel and structural members in reactors.<sup>1</sup> The fission process can result in localized zones of high thermal stress within a ceramic material.<sup>2</sup> A portion of the fission products are gaseous and radioactive; a ceramic such as a  $\text{UO}_2$  fuel element may become permeable during the fission process due to the introduction or opening of flaws by local thermal stresses. If this occurs, the radioactive fission products could rapidly develop a biologically dangerous discharge of radioactivity, or pressure build-up, within a material.

Complex ceramics are used as vacuum-tight envelopes in electronic devices. High-power pulses can cause rapid heating and cooling with resulting thermal stresses. If the ceramic material becomes permeable to gases under stress, the useful life of the device will be shortened.

In view of these facts, a study of the effect of stress on gaseous permeation through complex ceramics will furnish information useful in technical applications.

## A. Mathematics of Gaseous Permeation through Complex Ceramics

Solid-state volume diffusion of gas atoms through normally impermeable complex ceramics is usually the controlling step in the permeation process. A mathematical treatment of volume diffusion with a theoretical consideration of the effect of stress is given. It is possible that a Knudsen flow of gases through a ceramic could be induced by applying tensile stress; therefore, the introduction of Knudsen flow through induced stresses is discussed.

### 1. Volume Diffusion

Volume diffusion is the process of migration by which atoms or ions jump from one atomic site of low potential energy to another. When volume diffusion occurs, the potential field of the atoms or ions of the host material has a great influence on the diffusing species. Reviews of the derivation and solution of the diffusion equation have been published by Barrer,<sup>3</sup> and Jost.<sup>4</sup>

The mathematical approach to the problem of diffusion is the initial statement of Fick's first law of diffusion for steady-state conditions:

$$J = - D \frac{\partial c}{\partial x}, \quad (1)$$

where

$J$  = flux (atoms/unit time)/(unit area),

$D$  = diffusion coefficient ( $\text{cm}^2/\text{sec}$ ),

and

$\frac{\partial c}{\partial x}$  = concentration gradient in the direction of diffusion  
(atoms/ $\text{cm}^3$  cm).

Fick's first law will apply only if the conditions are satisfied that

- (a)  $J$  is proportional to the  $(\partial c/\partial x)$  at all concentrations,
- (b) There is no mutual interaction of diffusing species,
- (c) Concentration does not change appreciably in a single jump distance.
- (d) Interaction of the diffusing species with the solid is constant throughout the solid.

If Eq. (1) can be applied, an expanded form of it can also be used without much error to describe transient diffusion conditions. The expanded form of Eq. (1) is shown as Eq. (2).

$$\frac{\partial c}{\partial t} = D \frac{\partial^2 c}{\partial x^2}, \quad (2)$$

where

$$\frac{\partial c}{\partial t} = \text{change in concentration with time (atoms/cm}^3 \text{ sec),}$$

and

$$\frac{\partial^2 c}{\partial x^2} = \text{rate of change of concentration gradient (atoms/cm}^3 \text{ cm}^2 \text{)}.$$

For the steady-state flow of gases through a membrane, Darcy's law<sup>5</sup> can be stated

$$F = K\Delta PA/\Delta L, \quad (3)$$

where

$$F = \text{steady-state flow rate (atoms/sec),}$$

$$K = \text{permeation constant (atoms/cm-sec-atmos),}$$

$$\Delta P = \text{pressure differential across the membrane (atmos),}$$

$$A = \text{conducting area of membrane (cm}^2 \text{),}$$

and

$$\Delta L = \text{thickness of membrane (cm).}$$

K of Eq. (3) can be related to D of Eqs. (1) and (2) and a solubility coefficient (S) if the following assumptions are made:

(a) The concentration c follows Henry's Law, as shown in Eq. (4):

$$c = SP, \quad (4)$$

where

$$c = \text{concentration (atoms/cm}^3 \text{ of solid),}$$

$$S = \text{solubility coefficient, a constant of proportionality dependent on temperature only (atoms/cm}^3 \text{ atmos),}$$

and

$$P = \text{pressure of gas in equilibrium with concentration c of gas dissolved in solid (atmos).}$$

(b) D is a constant independent of concentration and dependent only on temperature.

- (c) The concentration at any point in the solid is an equilibrium one.
- (d) The volume diffusion process is the rate controlling process for passage of gas atoms through the membrane.

From Eq. (4) it follows that

$$\Delta P = \Delta c/S . \quad (5)$$

Equation (3) can be rewritten as

$$F/A = K\Delta c/S\Delta L . \quad (6)$$

Finally, comparison of Eqs. (6) and (1) shows that

$$K = DS, \quad (7)$$

where

$$F/A = J ,$$

and

$$\frac{\Delta c}{\Delta L} = \frac{\partial c}{\partial x}$$

If all the conditions mentioned previously are satisfied,  $K$  can be calculated by Eq. (3) from measurements of steady-state flow conditions.  $D$  may be calculated by Eq. (2) from the measurement of transient flow conditions. The solubility coefficient  $S$  can then be calculated by Eq. (7).

Physically,  $S$  is determined by the mechanism of solution of the gas atoms at the gas-solid interface:  $D$  is determined by the mechanism of transport of gas atoms through the material. The steps of solution and diffusion therefore determine the nature of the overall process of permeation as shown by Eq. (7).

Within experimental error it has been found that if volume diffusion is taking place, the following relationships are true:

$$D = D_0 \exp - [\Delta H_D/RT] . \quad (8)$$

$$S = S_0 \exp - [\Delta H_S/RT] \quad (9)$$

and

$$K = K_0 \exp - [\Delta H_K/RT] , \quad (10)$$

where

$\Delta H_D$  = activation energy of diffusion (cal/mole),

$\Delta H_S$  = activation energy of solution (cal/mole),

$$\begin{aligned}\Delta H_K &= (H_D + H_S) \text{ (cal/mole),} \\ R &= \text{gas constant (cal/mole } ^\circ\text{K),} \\ T &= \text{absolute temperature (} ^\circ\text{K),} \\ D_0 \text{ and } S_0 &= \text{constants for small concentration,}\end{aligned}$$

and

$$K_0 = D_0 \cdot S_0 .$$

The activation energy of diffusion is considered to be the average height of the potential energy barriers between solution sites. The activation energy of solution is considered to be the average potential energy barrier a gas atom must overcome in moving from the free gaseous state to a solution site in the solid.

## 2. Volume Diffusion in a Stressed System

The effect of stress on the overall permeation process is determined by the effect of stress on  $D$  and  $S$  individually.

Effect of Tensile Stress on  $D$ . The diffusion rate in a crystal or glass depends on the atomic interaction energy, and because this energy depends on interatomic distances it is to be expected that the diffusion coefficient of a migrating species will be altered by a strain imposed on the atomic lattice. In metal crystals, elastic strain can increase the self-diffusion coefficient by as much as a factor of 2.<sup>6</sup>

Girifalco and Grimes have developed a statistical rate theory for diffusion in strained crystals.<sup>7</sup> They show that the diffusion coefficient is an exponential function of strain. Furthermore, the strain effect can be represented by a parameter that is a function of interatomic forces. From their work, an expression can be developed for the diffusion coefficient of a strained lattice, as shown by

$$D_\epsilon = D(1 - \mu\epsilon_x)^2 \exp\left[\frac{M(1 - 2\mu)\epsilon_x}{kT}\right], \quad (11)$$

where

$$\begin{aligned}D_\epsilon &= \text{strained diffusion coefficient,} \\ D &= \text{unstrained diffusion coefficient,} \\ k &= \text{Boltzman's constant,}\end{aligned}$$

$\epsilon_x$  = strain in the  $x$  direction,

$\mu$  = Poisson's ratio,

$M$  = function of  $\partial\phi/\partial\epsilon_x$ ,

and

$\phi$  = potential energy of the system (a function of the 6 strain components as well as the atomic coordinates).

Girifalco and Grimes show further that their expression for  $D_\epsilon$  explains certain experimental data for self-diffusion in strained metal crystals. However, Sucov, on theoretical grounds, considers their value of  $D_\epsilon$  to be a lower limit for diffusion of oxygen through strained fused silica.<sup>8</sup>

Effect of Tensile Stress on  $S$ . In the permeation of noble gas atoms through a glass or crystalline lattice, it seems physically reasonable to assume that a decrease in diameter of the diffusing species would have the same relative effect on  $D$  and  $S$  as an expansion of the atomic structure under tensile stress.

Swets et al.,<sup>9</sup> and Barrer,<sup>3</sup> report data for helium, neon, and argon diffusion through silica. Solubility is found to vary by about a factor of 2 between the different gases, whereas  $D$  varied by at least two orders of magnitude. In fact, values of  $K$  for permeation of inert gases in glass afford a fairly good relative measure of  $D$  values.<sup>5</sup>

There is little conclusive evidence concerning the effect of inert-gas atomic size on  $D$  and  $S$  for gaseous diffusion through crystals. However, the effect should be approximately the same as in glass, since essentially the same mechanisms of solid-state solution and diffusion occur.

Effect of Tensile Stress on  $K$ . A tensile stress induced in a system through which an inert gas is diffusing would be expected to influence  $K$  of the diffusing species by a change in  $D$ , while  $S$  remained essentially constant.

Experimentally, it is usually easier to measure the effect of stress on  $K$ . Considering the previous discussion of the effect of stress

on D and S, an expression for K in a system strained in tension can be written as

$$K_{\epsilon} = S \cdot D (1 - \mu \epsilon_x)^2 \exp [ (M/kT) (1 - 2\mu) \epsilon_x ] , \quad (12)$$

where

$K_{\epsilon}$  = strained permeation coefficient, and  $k$  = Boltzman's constant.

Consideration of Eqs. (8), (9), (10), and (12) shows that tensile stress affects K by an effective change in the activation energy of diffusion.

The ratio of the strained and unstrained permeation coefficients is represented in

$$\frac{K_{\epsilon}}{K} = (1 - \mu \epsilon_x)^2 \exp [ M(1 - 2\mu) \epsilon_x ] / kT. \quad (13)$$

It follows that

$$\ln \frac{K_{\epsilon}}{K} (1 - \mu \epsilon_x)^{-2} = [ M(1 - 2\mu) \epsilon_x ] / kT . \quad (14)$$

In ceramic systems under stresses much less than Young's modulus, the term  $(1 - \mu \epsilon_x)$  approaches unity. Consequently, the influence of this factor is usually negligible and may be deleted, as shown in

$$\ln \frac{K_{\epsilon}}{K} = [ M(1 - 2\mu) (\sigma_x / E) ] / kT , \quad (15)$$

where

$$\frac{\sigma_x}{E} = \epsilon_x ,$$

and  $E$  = Young's modulus at the temperature of interest,  
 $\sigma_x$  = stress in the  $x$  direction (psi).

If Eq. (15) is valid, and the effect of stress on gaseous volume diffusion through a complex ceramic is due to homogeneous changes in interatomic distance, a plot of

$$\ln \frac{K_{\epsilon}}{K} \text{ vs } [ (1 - 2\mu) \sigma_x ] / ET$$

should result in a straight-line relationship. The line should pass through the origin with a slope equal to  $M/k$ .

3. Stress-Induced Knudsen Flow: Knudsen flow occurs when connected channels exist and the mean free path of a gas atom is much larger than the diameter of the channels. It is possible that Knudsen flow may be introduced into a system by applied tensile stress. Non-stress-bearing surfaces may separate to produce gas-conducting channels, and the surfaces may join again upon release of stress. A Knudsen flow of gases would exist only in the stressed condition.

In a material as described above, in a temperature range in which the elastic modulus does not change rapidly, equal stress levels at different temperatures should result in approximately equal-sized flow channels. Knudsen flow is directly proportional to  $T^{1/2}$ .<sup>5</sup> Therefore, a linear relationship should be found experimentally between the difference in flow rate in stressed and unstressed states, and  $T^{1/2}$ .

#### B. Earlier Experimental Investigations

The influence of stress on helium permeation of pyrex glass has been studied by McAfee.<sup>10</sup> He concluded that diffusion in glass proceeds along internal surfaces or voids for a considerable distance, but he did not rule out the chance of volume diffusion occurring along part of the path of the gas atom.

McAfee based his conclusions on experiments in which he found that large tensile stresses gave increased  $D$  above what would be expected for homogeneous expansion of the glass lattice with hard sphere interaction between atoms. Compressive stress did not show this behavior. His glass model for diffusion under stress thus consisted of randomly oriented submicroscopic flaws or voids, separated by narrow necks.

McAfee pointed out that the stress dependence of diffusion need not arise solely from change in activation energy with dilation of glass network. However, it was not possible to express strain dependence entirely within  $D_0$  as a change in jump distance between solution sites.

Studt has reported that changes in stress have induced intermittent flows of helium at room temperature in high-purity polycrystalline alumina.<sup>11</sup> The channels opened were evidently of atomic size along grain boundaries connecting isolated pores. Continued application of cyclic stress of constant stress level resulted in a gradual reduction and halt of the observed effect. Increasing the stress level again initiated intermittent flow with the same gradual reduction.

It was postulated that adsorption of gas atoms on the surface of microcracks eventually plugged channels, resulting in a decrease in flow even under cyclic stress conditions.

Previous experimental studies of the effect of tensile stress on gaseous permeation of ceramic materials have involved either a glass ceramic, or a complex one with very little glassy phase. Furthermore, these studies have been carried out at room temperature.

## II. EXPERIMENTAL PROCEDURE

It was reasoned that a permeation experiment which allowed variation in temperature would aid in distinguishing the mechanisms of gaseous permeation in stressed and unstressed ceramics, and that a variation in microstructure would help to establish a relationship between stress, microstructure, and gaseous permeation.

An experiment was designed and conducted which measured the influence of tensile stress and temperature on helium permeation through fused silica and complex ceramics of four different microstructures.

The stress dependence of the flow of helium through the walls of fused silica, high alumina, and refractory mullite tubes was investigated by mechanically subjecting them to longitudinal tensile stresses. Helium was selected for the diffusing gas because it is inert and during permeation would act essentially like a free atom.<sup>10</sup> In addition, helium would be the most likely of the inert gases to give a measurable flow rate because of its relatively small size.

The loading apparatus was designed so that the specimens were gripped at the ends and a uniaxial tensile load applied. Between the grips a molybdenum-wound resistance furnace maintained the test section of the tube at the desired temperature. Tests were conducted between room temperature and 1000°C. Either a vacuum or a helium atmosphere could be maintained in the furnace.

Gaseous flow through the wall of the specimens was detected by a mass spectrometer that continuously monitored the partial pressure of helium inside the tube. Continuous monitoring of the flow rate through the specimen allowed observation of any rapid changes that might accompany either transient stress conditions or flow under static conditions. Permeability characteristics could be determined from observation of steady-state and transient conditions of gaseous flow.

## A. Specimens

### 1. Composition and Physical Properties

Two commercially prepared high-alumina materials, designated alumina 1 and 2, two refractory mullite materials, designated mullite 1 and 2, and pure fused silica were selected for study. One firm supplied one alumina and one mullite sample, a second firm supplied the other two, and a third firm supplied the fused silica. All specimens were 9-in. -long tubes about 1/2-in. -o. d. and 3/8- or 1/4-in. i. d.

X-ray examination showed the presence of alumina and mullite in mullite 1, but only mullite in mullite 2. Pertinent chemical and physical properties of these five materials are given in Tables I and II.

Alumina and mullite specimens were chosen because of the relative importance of those two refractory ceramics in industry. In addition, the material was available commercially in the proper configuration with a wide selection of microstructures. Fused silica was studied because silica is usually a major constituent in the glassy phase of complex ceramics.

### 2. Specimen Preparation

Investigation of the qualitative temperature- and stress-dependence of gaseous diffusion was carried out on all specimens as they were received from the manufacturer. In addition, alumina 2 and mullite 1 were modified to obtain data enabling calculation of the diffusion coefficient, and stressed and unstressed permeation coefficients. The specimen configurations are shown in Fig. 1.

The modification of specimens was governed by three requirements:

- (a) The area of significant gaseous permeation had to be well defined.
- (b) The area of permeation had to be at a constant temperature.
- (c) Stress levels in the zone of diffusion had to be several times that of the adjacent portion of the specimen.

Table I. Physical properties of materials

	Apparent density <sup>a</sup> (g/cc)	Porosity		E (psi×10 <sup>6</sup> )	μ	Flexural strength, room temp. (psi×10 <sup>3</sup> )
		Closed <sup>a</sup> (%)	Open <sup>a</sup> (%)			
Alumina 1	3.77	6	nil	35 <sup>b</sup>	—	29 <sup>b</sup>
Alumina 2	3.69	6	nil	—	—	45 <sup>b</sup>
Mullite 1	2.44	18	nil	—	—	20 <sup>b</sup>
Mullite 2	2.74	13	nil	13 <sup>b</sup>	—	13 <sup>b</sup>
Fused silica	2.21	0	0	10.6 <sup>c</sup>	0.17 <sup>c</sup>	—

<sup>a</sup>Determined using a Beckman 930 air comparison pycnometer, accuracy ±0.05 cc; laboratory balance, accuracy ±0.0001 g; and a mercury-displacement volumeter.

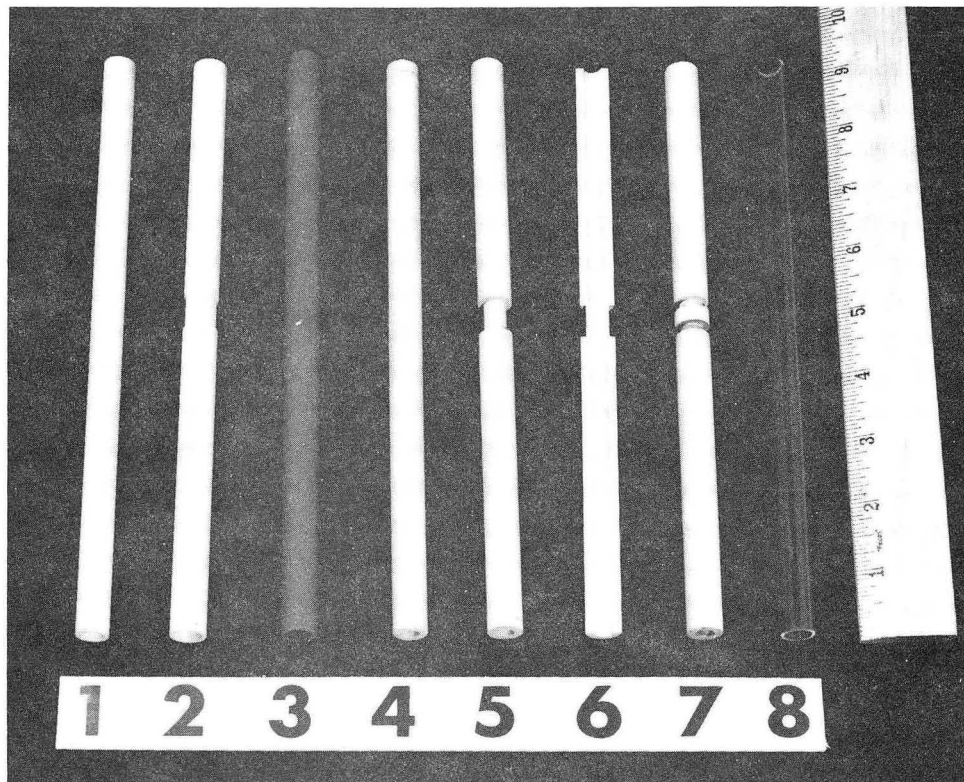
<sup>b</sup>Values as given by the manufacturer.

<sup>c</sup>See reference 18.

Table II. Chemical composition of materials, by weight percent<sup>a</sup>

Compounds	Alumina 1	Alumina 2	Mullite 1	Mullite 2	Fused silica
Al <sub>2</sub> O <sub>3</sub>	99.7	95.2	54	58.9	—
SiO <sub>2</sub>	0.2	4.0	43	36.5	100
Fe <sub>2</sub> O <sub>3</sub>	—	0.2	↑	0.9	—
TiO <sub>2</sub>	—	—	↑	1.2	—
NaO	0.1	0.1	3	1.2	—
CaO	—	0.2	↓	1.1	—
MgO	—	0.3	↓	0.4	—

<sup>a</sup>Chemical analysis as furnished by manufacturers.



ZN-3727

Fig. 1. Specimens: (a) alumina 1; (b) alumina 2 (modified)\*; (c) mullite 2; (d) mullite 1 (unmodified); (e) mullite 1 (modified); (f) mullite 1 (modified) showing longitudinal cross section of specimen with a test section at the center; (g) mullite 1 (modified) showing specimen with 1/2 the area of test section and twice as many fillets as the normal modified specimen; (h) clear fused silica. "Modified" implies the grinding of a test section (see text).

It is also important that the furnace had a relatively constant-temperature zone for about a half-inch along the axis in the center.

Specimens of alumina 2 and mullite 1 were modified by placing them in a lathe and grinding a reduced section with a diamond saw over a half-inch length. The reduced section was centered in the constant-temperature zone. The thin-walled section had a thickness of about 0.025 in. in alumina 2, and 0.040 in. in mullite 1. This section is hereafter referred to as the test section.

Sharp fillets were produced at the ends of the test section. The effect on permeation of the stress concentration at the fillet was investigated in mullite 1. The test section was prepared as described above, except that a 1/4-in. -long portion of unground tube was left in the center of the normal 1/2-in. test section. This produced a specimen with essentially half the area of a modified tube but twice as many fillets (see Fig. 1). If the stress concentration at the fillet contributed a significant amount to the measured permeation, it could be detected by comparison of data obtained from specimens of the two different configurations.

Results of permeation tests of modified specimens were compared with results from unmodified specimens. This comparison determined whether machining had significantly changed the permeation properties by introduction of flaws. In addition, it determined whether there was a relationship between the stress dependence of permeation and the wall thickness. Table III shows the dimensions of specimens used in the investigation.

### 3. Microstructure

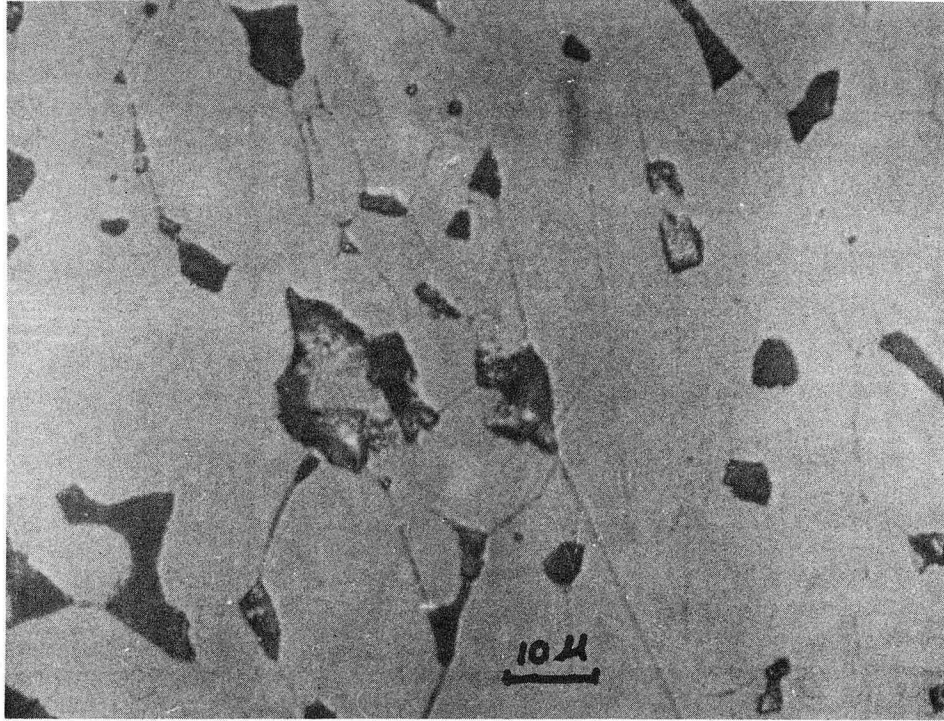
Metallographic studies were made on the alumina and mullite materials. All were polished on a diamond lap, and alumina 1 and 2 were then etched with orthophosphoric acid for three minutes at temperatures between 190 and 240°C. Mullite 1 and 2 were etched with a boiling 2% sodium carbonate solution. All specimens were then metalized with gold to render surface detail visible in the photomicrographs (Figs. 2 through 5). Straight dark lines extending across several grains are surface scratches resulting from preparation of the specimens.

Table III. Dimensions of specimens<sup>a</sup>

Material	Specimen designation	O. D. as received (in.)	I. D. (in.)	Wall thickness as received (in.)	Wall thickness of test section (in.)	Length of test section (in.)	Inside area of test section (in. <sup>2</sup> )	Cross sectional area (in. <sup>2</sup> )
Alumina 1	M1 <sup>b</sup>	0.5	0.31	0.08	—	—	—	0.10
Alumina 2	AV1B	0.5	0.384	0.06	0.037	0.500	0.621	0.049
	AV6B	0.5	0.380	0.06	0.036	0.500	0.596	0.047
Mullite 1	MT1	0.5	0.255	0.12	0.038	0.500	0.398	0.031
	MT2	0.5	0.254	0.12	0.037	0.500	0.397	0.034
	MT3	0.5	0.254	0.12	0.037	0.500	0.397	0.035
	MT4	0.5	0.253	0.12	0.038	0.500	0.396	0.035
	MTS1	0.5	0.254	0.12	0.039	0.250	0.199	0.037
	MTS2	0.5	0.257	0.12	0.038	0.250	0.201	0.035
	MT7 <sup>b</sup>	0.5	0.252	0.12	—	—	—	0.148
Mullite 2	MM3 <sup>b</sup>	0.511	0.371	0.070	—	—	—	0.097
	MM4 <sup>b</sup>	0.512	0.372	0.070	—	—	—	0.098
Fused silica	S1 <sup>b</sup>	0.490	0.410	0.040	—	—	—	0.056
	S2 <sup>b</sup>	0.483	0.403	0.040	—	—	—	0.055

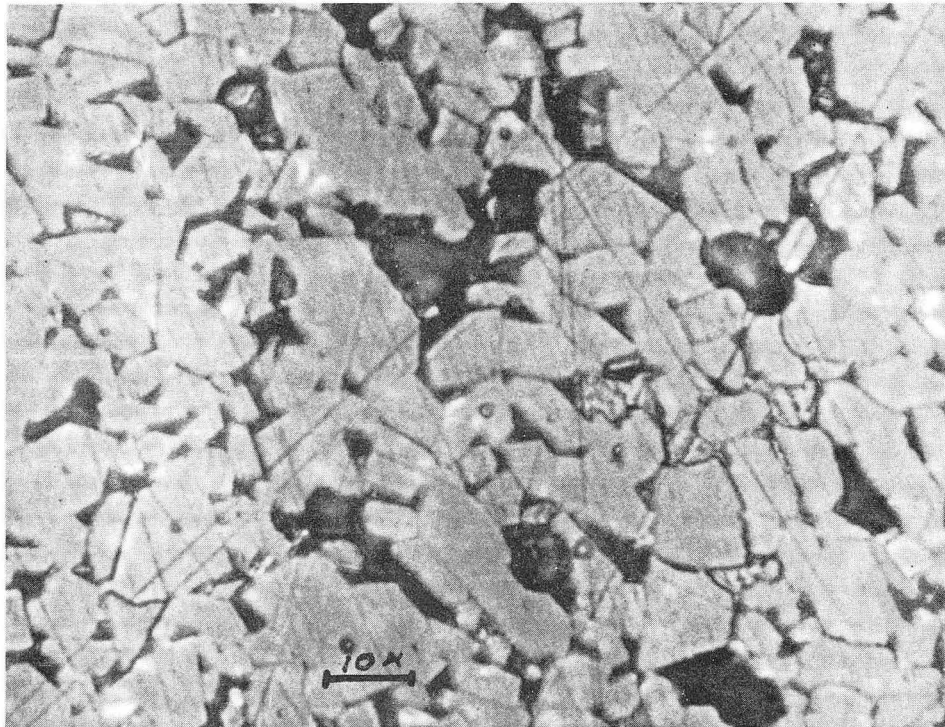
<sup>a</sup>All specimens were 9 in. long.

<sup>b</sup>No test section ground on tube.



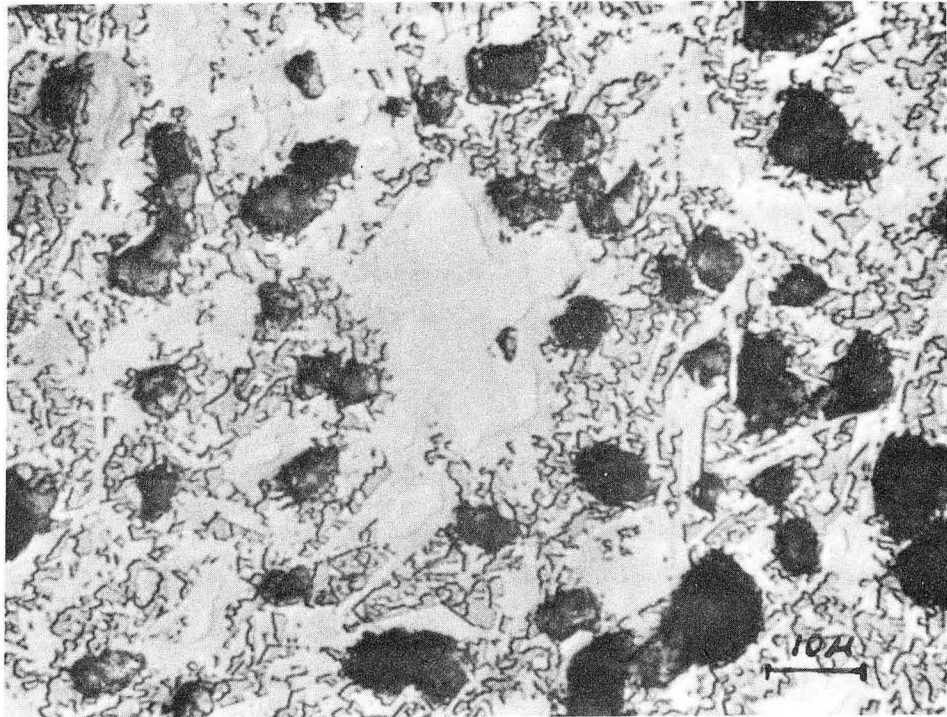
ZN-3725

Fig. 2. Photomicrograph of alumina 1 showing grain and pore structure. (870X)



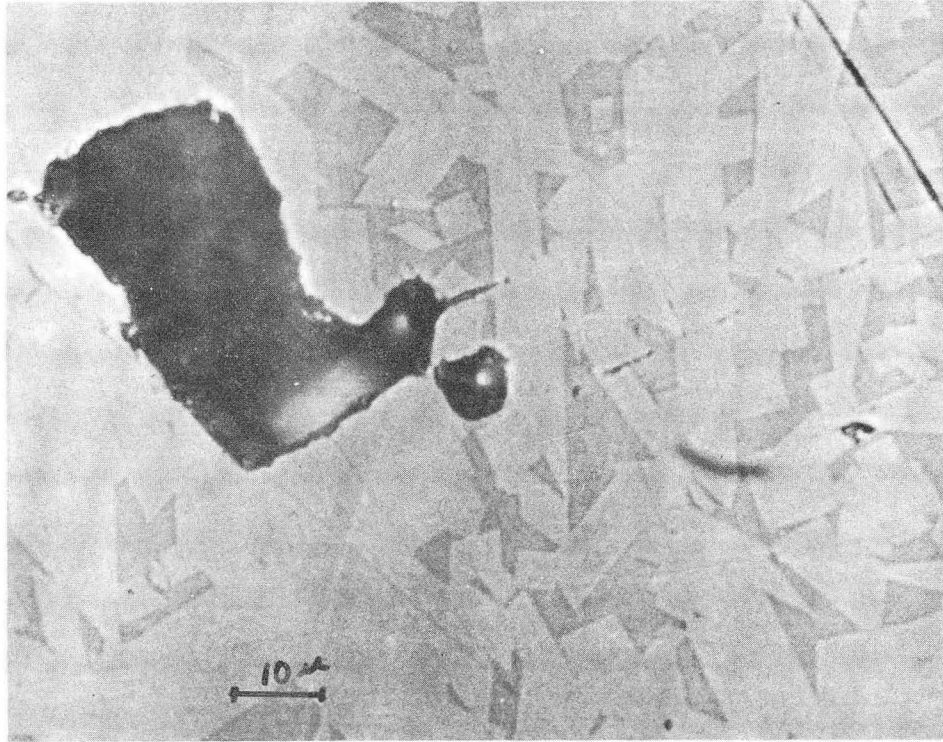
ZN-3723

Fig. 3. Photomicrograph of alumina 2 showing grain and pore structure. (870X)



ZN-3722

Fig. 4. Photomicrograph of mullite 1 showing grain and pore structure. (1040X)



ZN-3724

Fig. 5. Photomicrograph of mullite 2 showing grain and pore structure. (870X)

Alumina 1. Porosity exists at the intersection of most grain boundaries. Pores are several times smaller than the grain size. A small amount of glassy phase can be seen between some of the grains.

Alumina 2. Extensive porosity exists and pores are about the same size as the alumina grains. Alumina grains appear separated by a glassy phase. Pull-out of the glassy phase during polishing of the specimen probably caused some of the void areas between grains.

Mullite 1. In addition to extensive porosity, at least three phases are present in this material. The flat wide areas, such as the one in the center of the figure, are unreacted alumina. The darker phase surrounding the alumina is probably a mullite matrix. Needlelike crystals in the glassy matrix are probably mullite. Surrounding the mullite needles are areas of high-silica glass.

Mullite 2. Pore size was about the same as in mullite 1 although only one large pore is shown in Fig. 5. The overall porosity was less (see Table I). Well-developed lath-like crystals of mullite are visible in a glassy matrix.

## B. Apparatus

A schematic diagram of the arrangement of the apparatus is shown in Fig. 6. An overall view of the equipment is shown in Fig. 7.

### 1. Loading arrangement

An essentially uniaxial tensile load was transmitted from a mobile steel pressure plate to the specimens through a self-aligning device that minimized stress concentration at the grips. The grip consisted of two parts. The first part was a hardened steel hemisphere, resting on steel balls in a socket around a 5/8-in. hole in the pressure plate. The second part was a 1/2-in. long copper collar with a 3/4-in. o. d. The i. d. was sized so it could be slipped over the specimen with a 1/16-in. clearance.

A collar was fastened to each end of the tube with epoxy epone resin. When the specimen was in loading position, each end passed through the center of a pressure plate and steel hemisphere. Load was

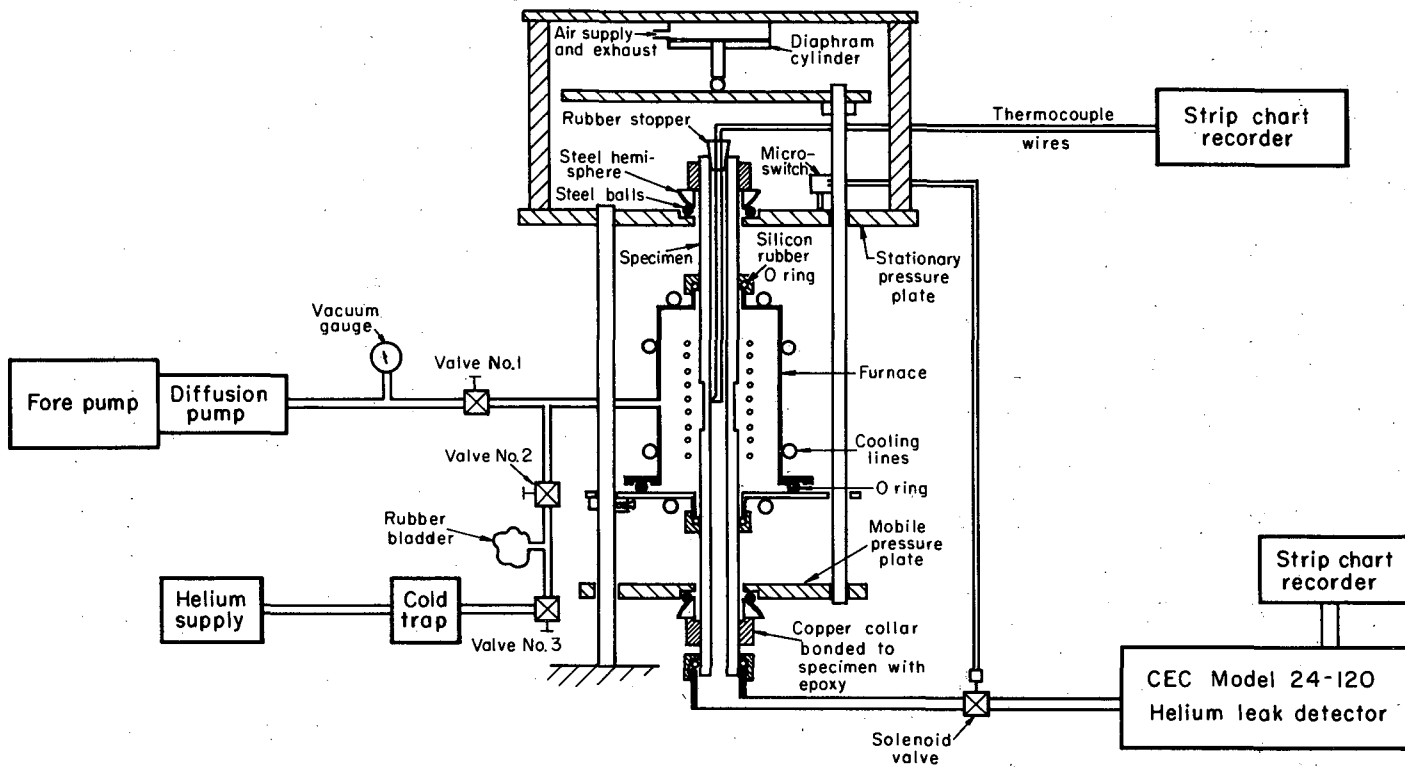
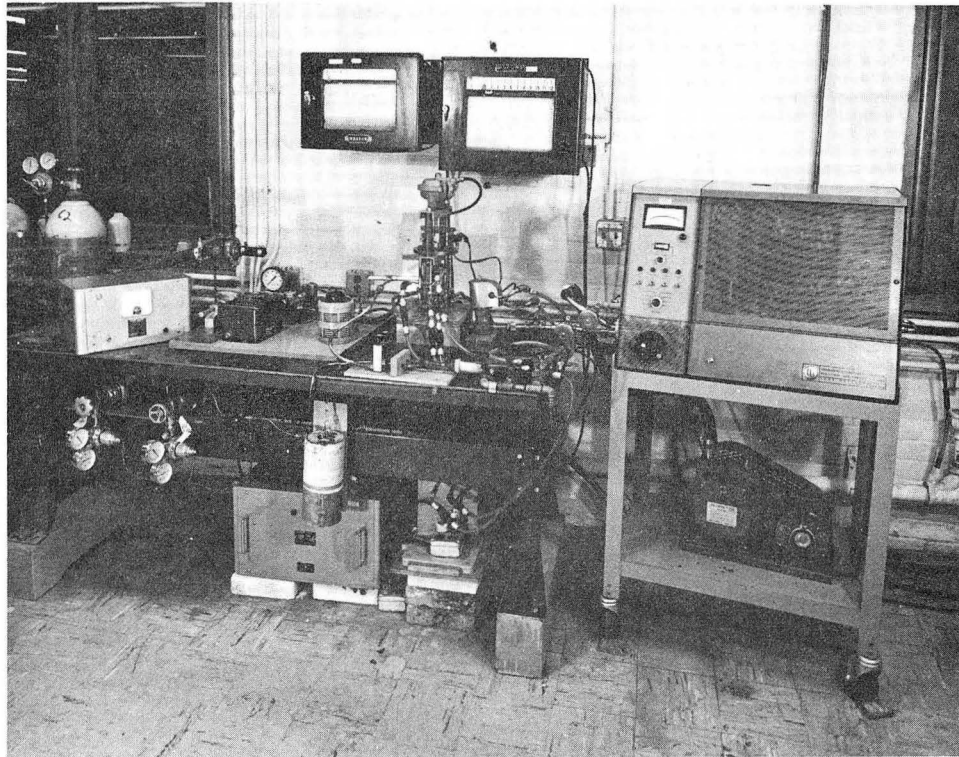


Fig. 6. Schematic representation of the apparatus.



ZN-3729

Fig. 7. Overall view of the apparatus.

applied by moving one pressure plate relative to the other. The flat portion of the hemisphere in the pressure plate made contact with the copper collar at each end and loaded the specimen in tension. Any slight misalignment of the copper collar or pressure plate was corrected by movement of the hemisphere.

Loads were applied to the pressure plates and hence to the specimen by means of a diaphragm cylinder actuated by air pressure. Air pressure introduced into the diaphragm cylinder was controlled by a pressure regulator. Loads available with the diaphragm cylinder were from 0 to 765 lbs. Figure 8 shows the apparatus assembled with the specimen in place.

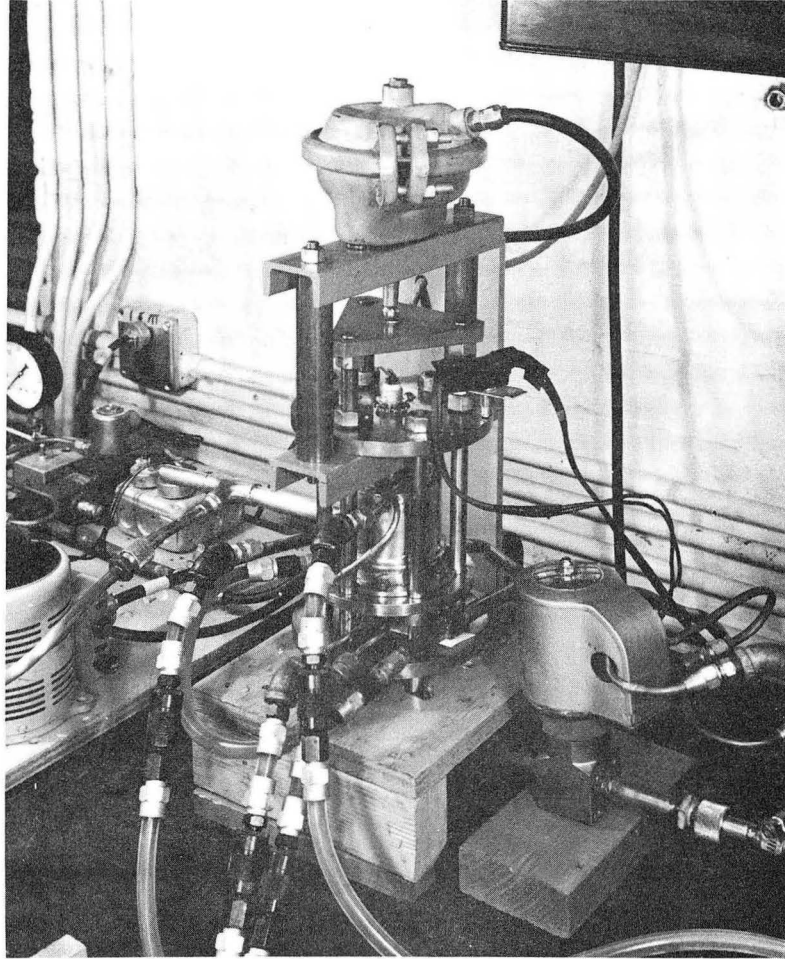
## 2. Cycling Arrangement

The load could be applied and removed by means of time switches and an electric solenoid valve on the pressure line leading to the diaphragm cylinder. A schematic of the cycling arrangement is shown in Fig. 9. The length of time for load application, and time between loading, was set independently on the timer. Each of these time intervals was variable from 15 seconds to 15 minutes. Therefore, a complete cyclic interval was available from 30 seconds to 30 minutes.

The rate of loading could be varied by a valve adjustment between the solenoid valves and the pressure regulator. Maximum loading rate was on the order of 0.1 sec. A minimum loading rate of several minutes could be obtained by manually adjusting the pressure regulator.

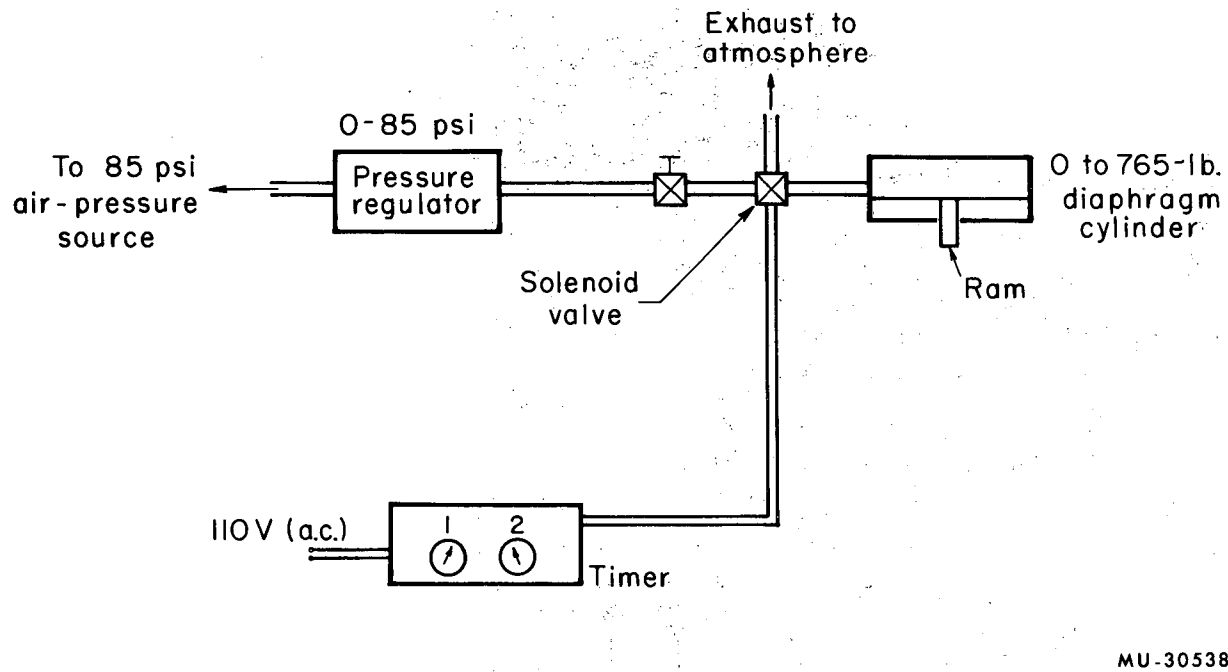
## 3. Furnace Arrangement

The furnace shell was constructed of brass and was water cooled. It rested on collars fixed to the steel legs supporting the stationary pressure plate. The heating element was a 2 1/4-in. -long coil of 0.090-in. -diam molybdenum wire. A relatively constant temperature zone existed for about 1/2 in. at the center of the coil at most operating temperatures.



ZN-3726

Fig. 8. Furnace and loading device assembled.



MU-30538

Fig. 9. Schematic representation of compressed-air supply, exhaust, and loading-control system.

The gap between the specimen and the furnace at the two ends was sealed by placing a silicon rubber "O" ring around the tube at each end of the furnace. By loosening the "O" ring, a specimen could be easily removed or placed in the furnace without further disassembling. Negligible stress was induced in the specimen by the "O" ring.

Figure 10 shows the furnace disassembled, with a specimen in the position it would normally occupy.

#### 4. Temperature Measurement

The temperature of the test section was measured by placing a Pt-Pt 10% Rh thermocouple in contact with the inside of the tube at the center of the furnace. The temperature gradient from the center  $\pm 1/4$  inch was found to be about  $10^{\circ}\text{C}$  with helium in the furnace.

The thermocouple wires were led out through a rubber stopper at one end of the specimen and then to a strip chart recorder.

#### 5. Power Supply

The temperature at any point in the furnace was maintained within  $\pm 2^{\circ}\text{C}$  during a run by providing a constant voltage to the coil, and cooling the furnace shell with constant-temperature water. Very stable low-voltage electric power was supplied to the furnace by means of a voltage stabilizer, a manually controlled auto transformer, and a 20-to-1 step-down transformer.

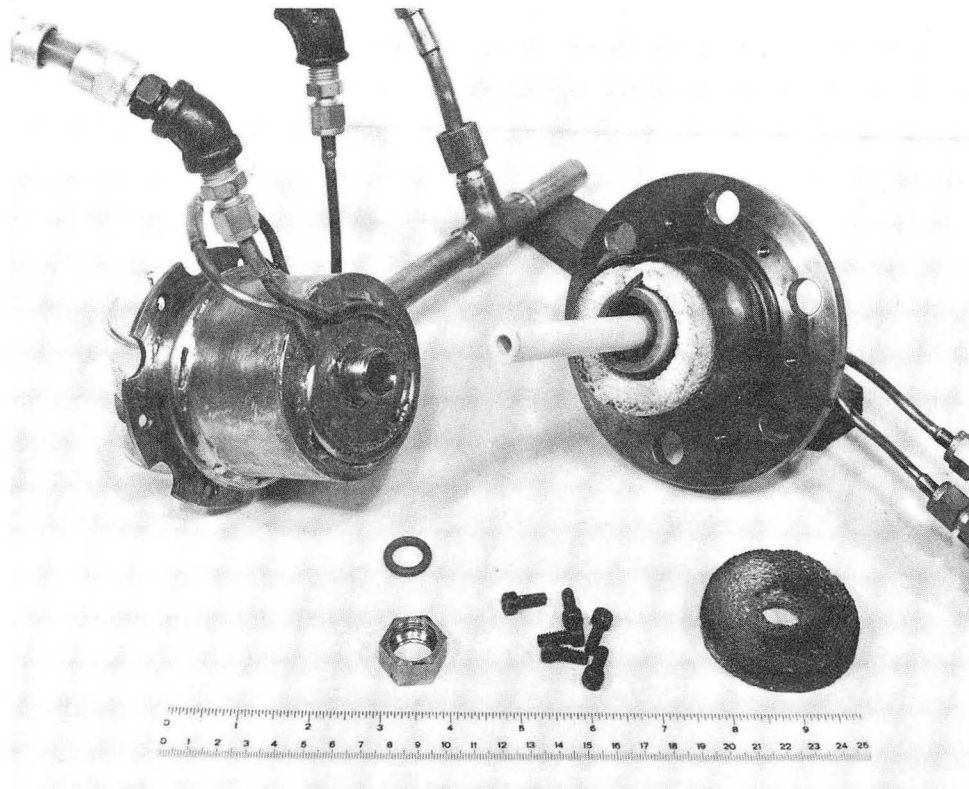
#### 6. Atmosphere Control

The atmosphere of the furnace could be maintained at a vacuum of  $10^{-4}$  Hg, or 1 atmos of helium.

An oil diffusion pump was used to evacuate the furnace, and an ionization gauge measured the pressure. One atmosphere of helium could be supplied to the furnace by means of the system shown in Fig. 6.

#### 7. Flow Rate Measurement

A Consolidated Electrodynamics (CEC) leak detector, Model 24-120 was used to measure gas flow through the specimen. All gas passing through the tube walls passed through the leak detector.



ZN-3728

Fig. 10. Furnace disassembled, showing specimen in place.

A sensitivity of from 1 to  $2 \times 10^{-10}$  atm-cc/sec div was normally achieved. Output of the instrument was recorded on a strip chart recorder.

The leak detector vacuum system was connected to the specimen by a 1-ft length of 1/2-in. copper tubing. Earlier use of a 4-ft length of tygon tubing gave unsatisfactory results because of the large volume and the resulting slow pump-out rate. The tubing was connected to the specimen at the lower end by a rubber "O" ring seal. An electric solenoid in-line vacuum valve was placed in the line between the specimen and the leak detector. It closed when the specimen broke and so protected the vacuum system of the leak detector.

#### 8. Calibration of Equipment

The air pressure gauge was calibrated in terms of load applied to tube specimen by the diaphragm cylinder. The loading device was fastened in place in an Instron Type TTCL machine with an autographic recorder. A compression-load cell measured load applied to the lower pressure plate as air pressure was varied in the diaphragm cylinder. The calibration curve obtained is shown in Fig. 20, Appendix A.

The leak-detector mass spectrometer was calibrated before and after each specimen was tested by using a helium source of known flow rate. The background for the mass spectrometer was determined, and then the helium source was vented to the instrument and allowed to reach steady-state flow. Sensitivity is given in the form of this flow rate per percent of recorder full scale, with the mass spectrometer on its most sensitive setting. Calculations for a typical calibration are shown in Appendix B.

### C. Test Procedure

All specimens were washed in hexane and rinsed with methyl alcohol before being used.

#### 1. Modified Specimens

Specimens of alumina 2 and mullite 1 which had a test section were first placed in the apparatus. The diffusion coefficient and permeation coefficient was determined for specimens that exhibited detectable permeation. The mathematics of the method is shown in Appendix C.

The data needed for a calculation of the diffusion and permeation coefficient was obtained by the following procedure. Valve 2 was closed and valve 1 was opened to evacuate the furnace to  $10^{-4}$  mm Hg (see Fig. 6). The furnace was then brought up to the test temperature. The leak detector monitored the inside atmosphere of the specimen until a steady background was established. This usually took several hours. Valve 1 was then closed, and 2 and 3 were opened to fill the furnace with helium. The rubber-bladder reservoir maintained 1 atmos pressure in the furnace after valve 3 was closed.

Furnace temperature was maintained at a constant  $\pm 5^{\circ}\text{C}$  upon introduction of helium by manually increasing the power input. A typical curve obtained when permeation was detected is shown in Fig. 22 of Appendix C. When the output of the leak detector, as recorded on the strip chart recorder, ceased to rise more than 1% of full chart deflection in 15 minutes, it was assumed that essentially steady-state conditions existed in the test section. Permeation of helium through the thick walls of the specimen on either side of the test section was still under unsteady-state conditions but was not considered significant. Therefore, the accuracy of the data was enhanced by minimizing flow through the thick portions of the specimens.

After steady-state permeation through the test section had been determined, valve 2 was closed and valve 1 opened, to evacuate

the furnace rapidly to  $10^{-4}$  mm Hg. The temperature was held within  $\pm 5^{\circ}\text{C}$  at the test temperature by manually decreasing the power supply to the furnace as helium was evacuated. After a short time, the flow rate decreased in a characteristic exponential decay curve. When the flow rate had decreased to less than 1% of full chart scale in 15 minutes, steady-state conditions were again assumed to exist. The data were correlated to compute the diffusion and permeation coefficients.

After D and K at several temperatures had been determined, the furnace was filled with helium at a set temperature. After 18 hours, a steady-state permeation existed in all parts of the specimen. The leak detector output did not change with time, and the zero point could then be electronically shifted to a more sensitive scale. The specimen was then subjected to a series of loading cycles.

Within the sensitivity of the apparatus, the change in permeation rate appeared to be instantaneous upon application or removal of load, and to reach equilibrium immediately. The change also appeared to be independent of the load rate and number of cycles applied. Therefore, the following standard loading cycle was adopted, which gave reproducible results.

The recorder-pen position was marked as the load was rapidly applied. In 30 seconds the pen position was again marked, and the load was rapidly removed. The difference between the two marked positions was taken as the difference in permeation rate in the stressed and unstressed states. The minimum signal-to-noise ratio which gave useable results was about 3. The maximum signal-to-noise ratio obtained was about 6. The change in permeation rate upon load removal was always within 10% of the value of the change upon load application, but showed more scatter. For this reason, only the values for the change of permeation upon load application were used in calculations.

The average value of the change in steady-state permeation for about 12 cycles at the same stress level was used to determine the stressed steady-state permeation rate. Values that deviated more

than 20% from the mean value were ignored. Usually, four different loads were applied at one temperature. If fracture did not occur, the temperature was changed, and after about 18 hours a new steady-state condition existed and another series of loads were applied. Finally, after runs at several temperatures, a series of higher and higher loads was applied until the specimen failed. The thickness of the test-section wall was then measured by a tube micrometer. Tensile stress levels induced during the tests were determined by dividing the load by the cross-sectional area.

## 2. Unmodified Specimen

Specimens with no test section were placed in the loading apparatus and the furnace evacuated to  $10^{-4}$  mm Hg. The furnace was brought to a set temperature and helium introduced. Steady-state permeation was attained in about 18 hours. Series of loading cycles were carried out at various temperatures in the same manner as with the modified specimens. Changes in permeation rate upon application and removal of the load were observed and recorded. Stress levels were determined as for specimens with test sections.

The effect of a loading rate slower than maximum was investigated in the case of each specimen by using loading rates of 15 seconds, 1 minute, 5 minutes, and 15 minutes, and observing the effect on permeation.

### III. EXPERIMENTAL RESULTS

#### A. Alumina 1 and 2

No permeation of helium through the alumina specimens was detected. One specimen of alumina 1 and two of alumina 2 were tested in the stressed and unstressed states. Test conditions and results are shown in Table IV, Appendix IV. The temperature was limited to 271°C or less for alumina 1, because the silicon rubber "O" rings melted at higher temperatures. Alumina 2 specimens had thinner walls and lower thermal conductivity, so that higher temperatures could be used.

#### B. Mullite 1

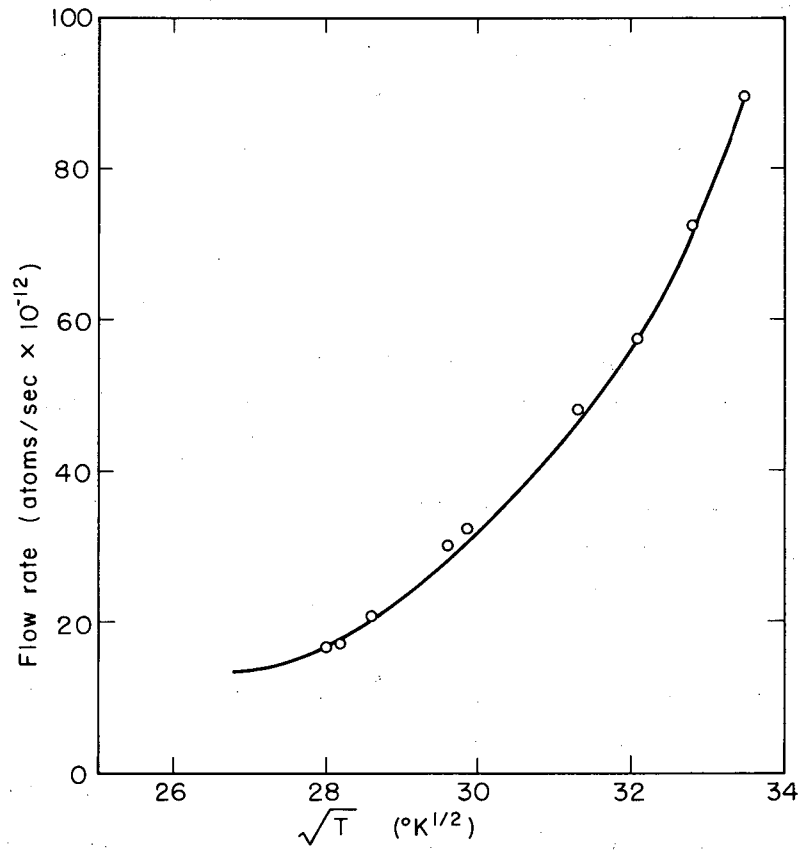
The modified specimen allowed the temperature to be determined through which the main bulk of diffusion was occurring. The absolute magnitude of the helium flow rate through the specimen wall versus  $T^{1/2}$  is plotted in Fig. 11. A nonlinear relationship was observed. Hence, Knudsen flow was determined to be insignificant in these specimens.

Logarithms of permeation coefficient  $K$  and diffusion coefficient  $D$  are plotted vs.  $T^{-1}$  in Figs. 12 and 13 respectively. The relationships are approximately linear, and straight lines have been drawn through the data points. Therefore, the flow of helium through the specimens appears to be predominately by volume diffusion. From the slope of the lines, the activation energies of permeation and diffusion were determined as 8550 and 9720 cal/mole respectively. From the intercept with the ordinate,  $K_0$  and  $D_0$  were obtained. The expression for the lines drawn through the data points of Figs. 12 and 13 are shown as

$$K = 12.90 \times 10^{13} \exp \left[ - \frac{8550}{RT} \right] \text{ atom/sec cm,} \quad (16)$$

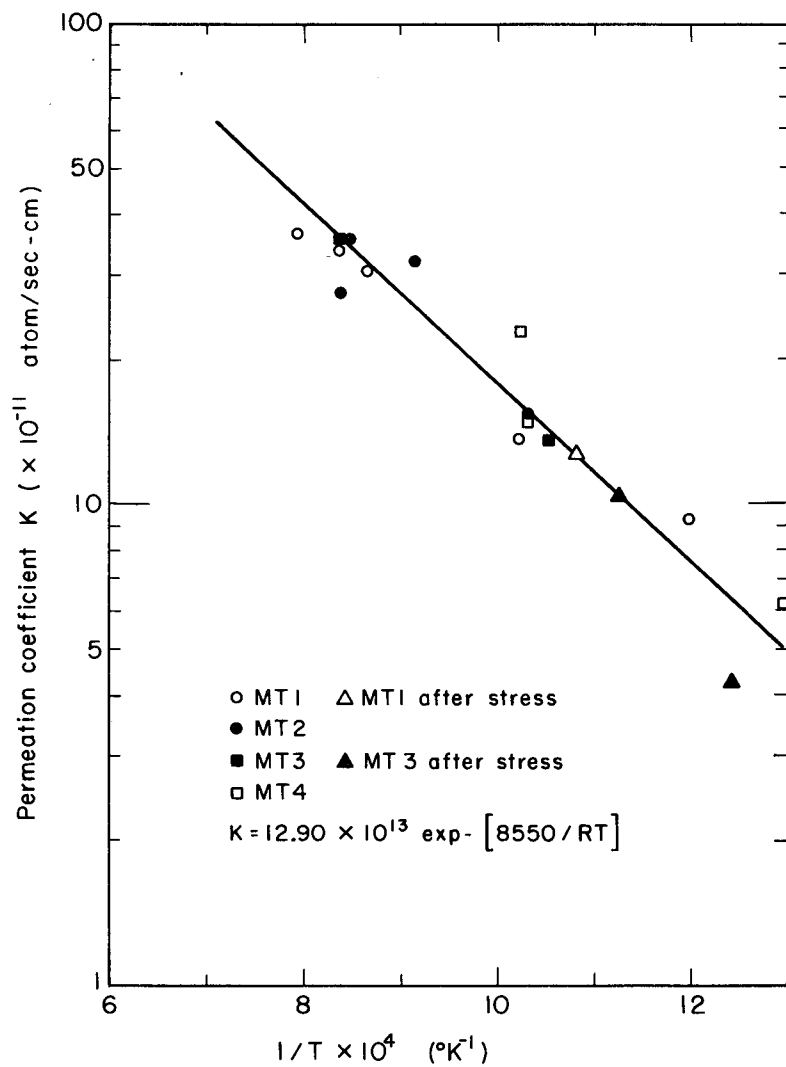
and

$$D = 1.55 \times 10^{-4} \exp \left[ - \frac{9720}{RT} \right] \text{ cm}^2/\text{sec.} \quad (17)$$



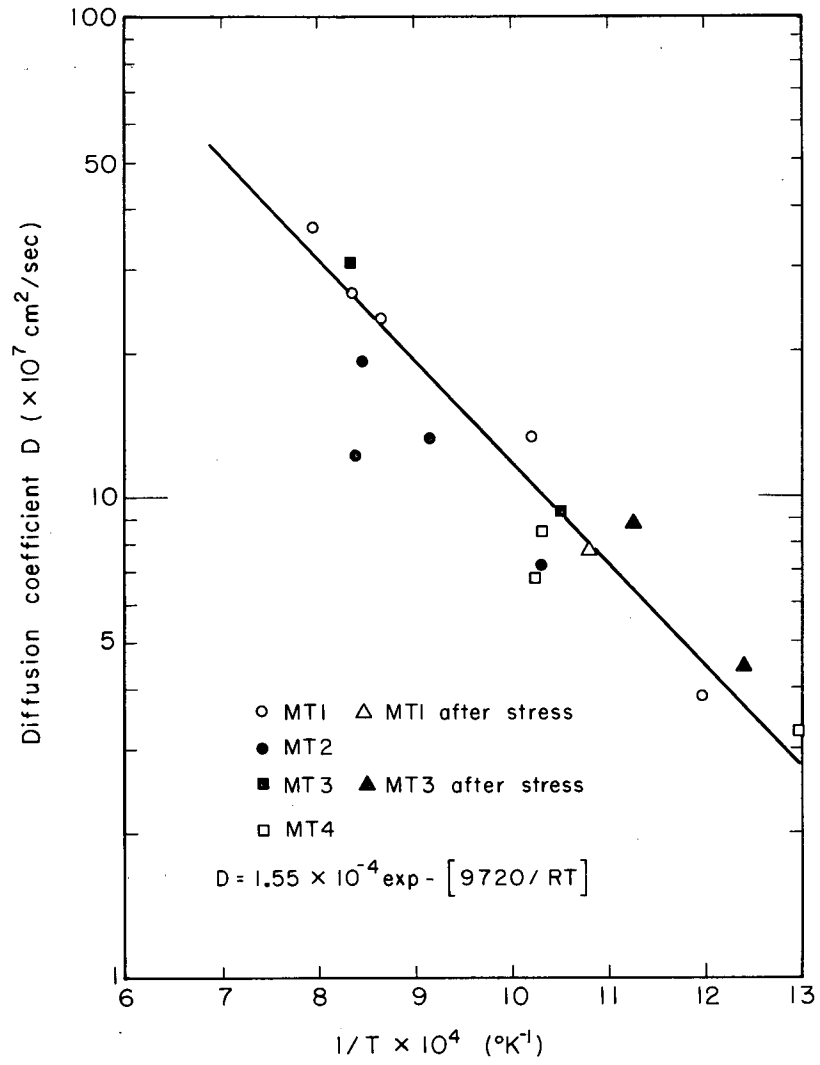
MU-30539

Fig. 11. Temperature dependence of flow for mullite 1.



MU-30540

Fig. 12. Temperature dependence of the permeability coefficient for mullite 1.



MU-30541

Fig. 13. Temperature dependence of the diffusion coefficient for mullite 1.

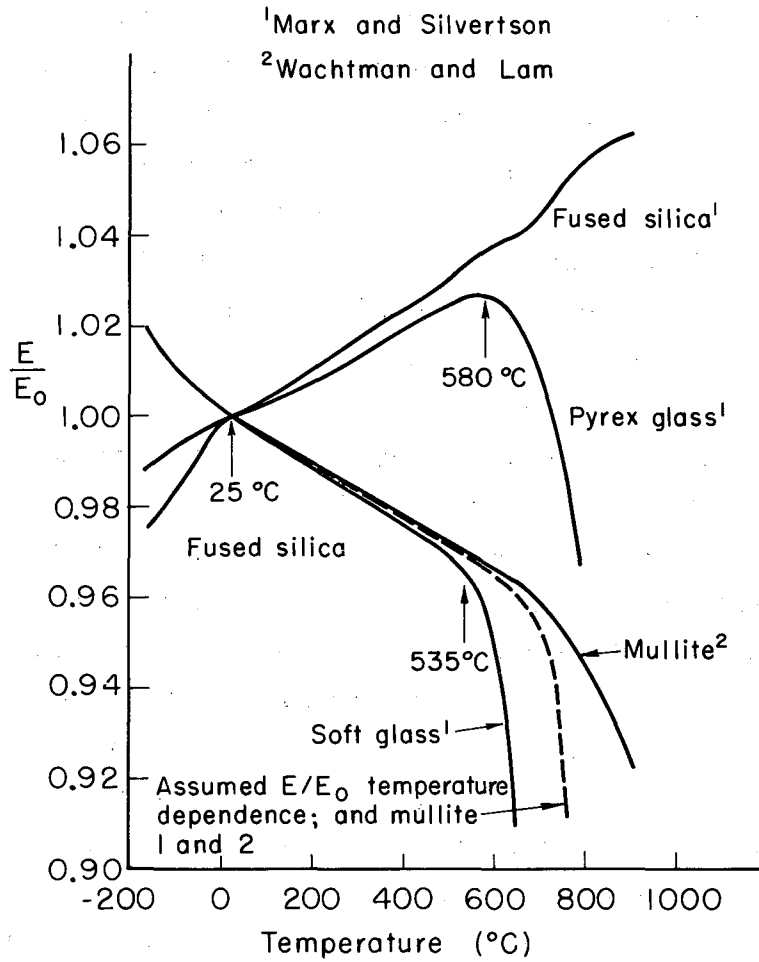
The most probable activation energy of diffusion and permeation, as shown in Eqs. (16) and (17), is what is expected for helium diffusion through glasses of high  $\text{SiO}_2$  content.<sup>12</sup> From knowledge of the chemical composition, x-ray diffraction patterns, and microphotographs it seemed reasonable that the glassy phase would have a high  $\text{SiO}_2$  content. It was therefore concluded that volume diffusion of helium through the glassy phase was the rate-controlling step, as is generally the case in polycrystalline multiphase ceramic materials.<sup>13</sup>

Four specimens of mullite 1 were tested under stress at temperatures between 511 and 852°C, and at stress levels between 1860 and 6160 psi. The change in flow rate upon application of equal stresses at different temperatures did not show a consistent  $T^{1/2}$  dependence. Therefore, the contribution to permeation by Knudsen flow in the stressed state was considered negligible.

Before the validity of Eq. (15) could be tested, the temperature dependence of Young's modulus of the material had to be determined. The temperature dependence of Young's modulus for refractory mullite has been determined by Wachtman and Lam using the dynamic method.<sup>14</sup> Dunsmore et al. used a static technique to determine the temperature dependence of elasticity (E) for two different kinds of mullite bodies.<sup>15</sup> Below 600°C the temperature dependence of elasticity as reported by the two investigations is not the same. However, an important fact is that both studies reported a rapid decrease in elasticity above 600°C for all specimens. The elasticity determined by the dynamic method is usually considered more accurate;<sup>16</sup> therefore, the work of Wachtman and Lam was used to analyze the data from mullite specimens in this study.

The temperature dependence of elasticity of soft glass, pyrex and fused silica has been reported by Marx and Silvertsen.<sup>17</sup> The fractional change in elasticity of mullite, soft glass, pyrex, and fused silica, as a function of temperature, has been plotted in Fig. 14.

The curve of the mullite temperature-dependence of  $E/E_0$  bears a striking resemblance to that of soft glass. The glassy phase of the



MU-30542

Fig. 14. Fractional change in Young's modulus as a function of the temperature for several ceramic materials.

mullite at the grain boundaries is considered responsible for the characteristic curve of the mullite.<sup>14</sup> The glassy phase of mullite would have a temperature-dependence of elasticity very similar to soft glass, but with a higher softening temperature. The higher softening point is reasonable in view of the higher  $\text{SiO}_2$  and lower alkali content of the glassy phase of the mullite bodies.

It was assumed that the Young's modulus of interest would be that of the glassy phase rather than of the entire polyphase ceramic, since the permeation rate-determining step was apparently volume diffusion through the glassy phase.

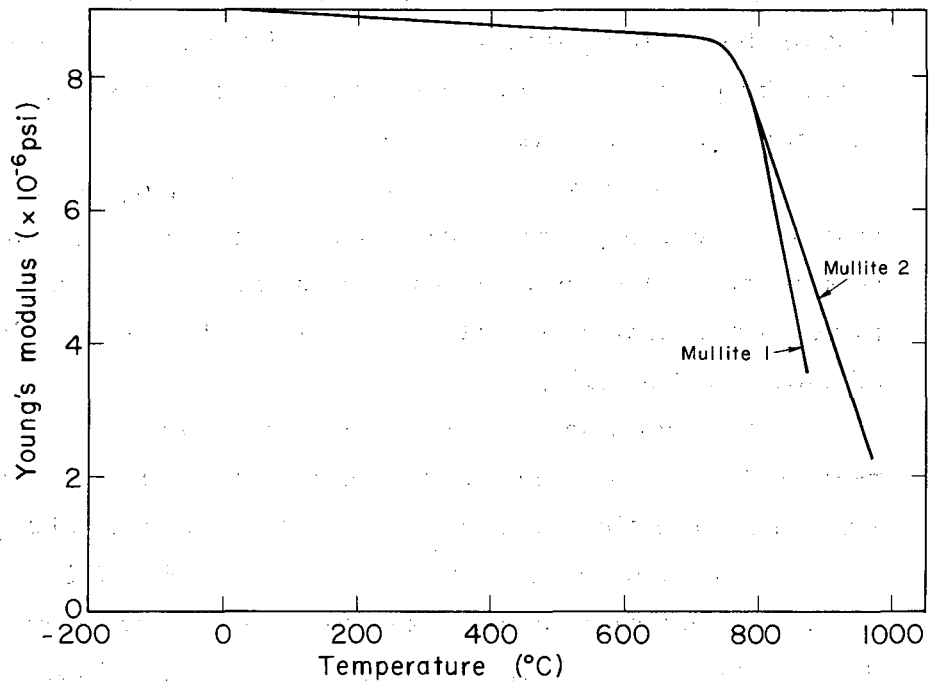
As an approximation to the elasticity of the glassy phase of mullite 1, a room temperature value typical for glass, of  $9 \times 10^6$  psi was chosen. The temperature dependence of elasticity was assumed to be as shown in Figs. 14 and 15, and this choice allowed correlation of data with Eq. (15).

The Poisson's ratio in the temperature interval of these experiments was approximated as 0.25. Poisson's ratio normally has a slight positive slope even when Young's modulus changes drastically.<sup>16</sup>

The value of  $K$  was obtained from Eq. (16).  $K$ , and the change in permeation rate, upon stress application, were used to calculate  $K_e$  by use of Eq. (34), Appendix C. The data from stress-dependence runs were then plotted as shown in Fig. 16. A line was drawn through the origin and along the apparent axis of the data points. The linearity of the plot shows that within experimental error the form of Eq. (15) is valid within the temperature and stress ranges used.

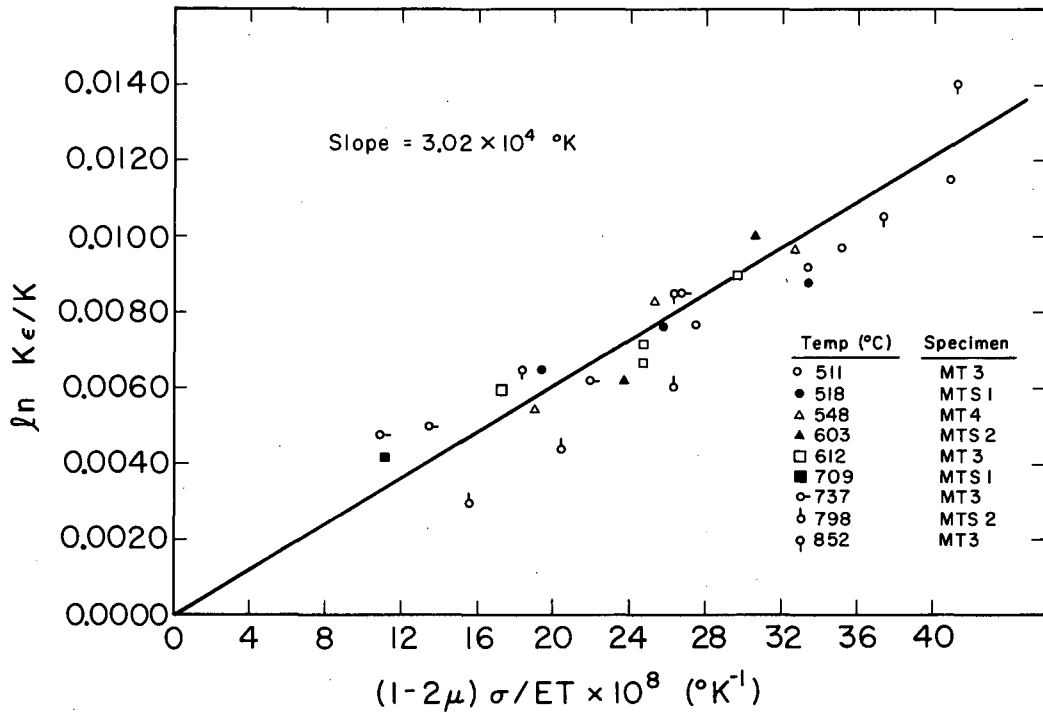
The stress concentration effects of the fillets did not contribute significantly to the observed phenomenon. The data from the specimens with half the normal area of test section, but twice as many fillets (MTS1 and MTS2), falls in well with data from normal specimens (see Fig. 16).

One unmodified specimen of mullite 1 was tested at various stress levels and temperatures. Temperatures between 553 and 866°C,



MU-30543

Fig. 15. Assumed Young's modulus temperature dependence for the glassy phase of mullite 1 and 2.



MU-30544

Fig. 16. Temperature and stress dependence of the permeability coefficient; mullite 1, modified specimens.

and stress levels between 1600 and 4820 psi, were used. For an equal stress level and temperature, the absolute magnitude of the stress effect was about one-fourth that observed in the modified specimens. Essentially the same relative stress effects were observed as with the modified specimens. The interpretation of data was difficult at lower temperatures and stress levels because the signal-to-noise ratio was about 3. Equation (15) was tested by plotting the data as shown in Fig. 17. Elasticity was assumed to vary with temperature, as shown in Figs. 14 and 15.

K was obtained by use of Eq. (34), Appendix C, where  $h_0$  was the total helium flow rate through the unstressed tube walls.  $K_e$  was obtained by the use of same equation, where  $h_0$  was the total flow through the unstressed walls, plus the additional flow ( $\Delta h$ ) caused by tensile stress. A line with a slope of  $2.08 \times 10^4$  °K was drawn through the origin and approximated the slope of the data points. The major error in the data points probably arises from the fact that a severe temperature gradient existed over the stressed portion of the tube. The temperature was measured at the hottest part of the specimen; that is, no attempt was made to find an average test temperature. The consistent use of a high value of temperature would cause the slope of the data of Fig. 17 to be less than that of Fig. 16. In view of the errors involved, the significance of Fig. 17 is that it shows tensile stress to have essentially the same characteristic effect, and to be of the same order of magnitude in the unmodified and modified specimens. The tabulation of data for mullite 1 is given in Table V, Appendix D.

### C. Mullite 2

Mullite 2 had diffusion characteristics similar to mullite 1, but was relatively more impermeable. The effect of tensile stress on helium permeation through two specimens was investigated. Temperatures between 685 and 939°C, and stress levels between 1650 and 4070 psi, were used. It was assumed that the controlling step in the permeation process was volume diffusion through the glassy phase, and this

phase was estimated to be about a 77%  $\text{SiO}_2$ . The elasticity was assumed to have the values and temperature dependence shown in Figs. 14 and 15 because of the reasons already discussed for mullite 1.  $K$  and  $K_\epsilon$  were determined by the same technique used for the unmodified specimens of mullite 1. The validity of Eq. (15) was tested by plotting the data (shown in Fig. 18). The tabulation of data is given in Table VI, Appendix D.

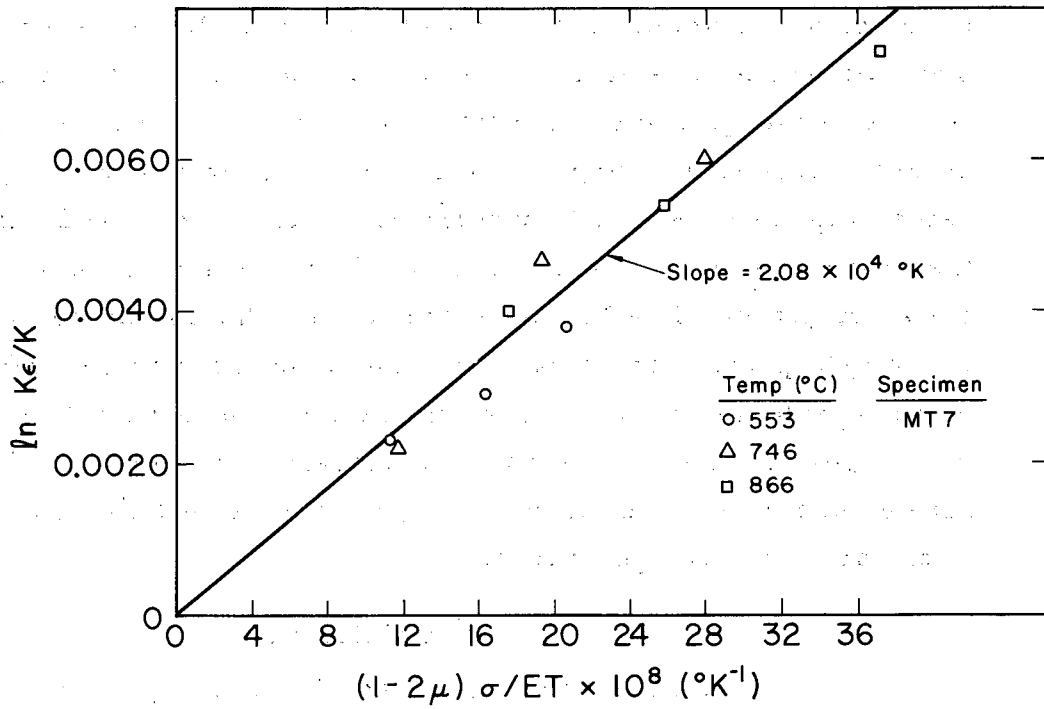
Essentially the same stress, temperature and elasticity dependences of the permeation were observed for mullite 2 as for mullite 1. The data are bracketed by two lines passing through the origin. There is a rather large scatter of data. The slopes of the limit lines differs by 59%. It is interesting that a line passing through the origin with the same slope as in Fig. 17 approximately bisects the band enclosed by the bracketing lines. Furthermore, data points of equal temperature show approximately a linear relationship. The major source of error in the data points was probably the same as for the unmodified mullite 1. The use of higher temperatures than were used for mullite 1 resulted in sharper thermal gradients. Consequently, the measured temperature values used to obtain the data points became less representative of the specimen temperatures.

#### D. Fused Silica

Volume diffusion through fused silica is reported in the literature<sup>19</sup> and was assumed to occur in these experiments.

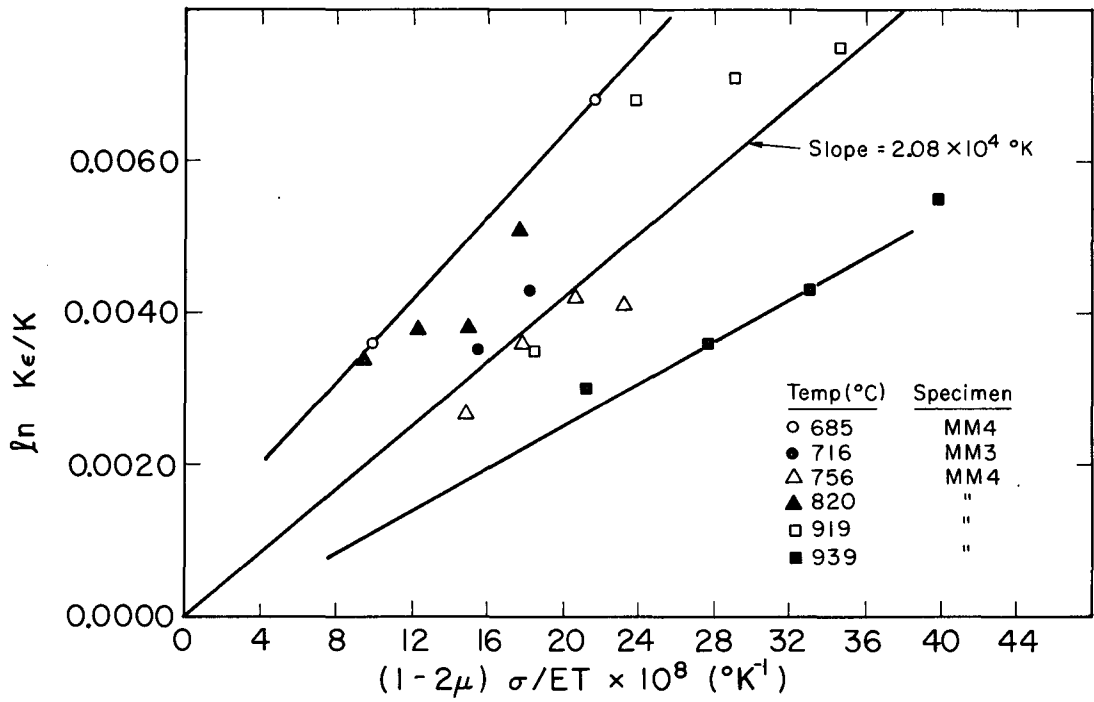
The validity of Eq. (15) was tested by plotting in Fig. 19 the data obtained from the two specimens tested. The room temperature value of elasticity equal to  $10.7 \times 10^6$  psi, and an average value of  $\mu$  equal to 0.17, were chosen from reference 16. Figure 14 shows the temperature dependence of the modulus of elasticity.

Lower temperatures were necessary for tests on fused silica because it is relatively permeable to helium, and it was necessary for all of the diffusing gas to pass through the mass spectrometer.



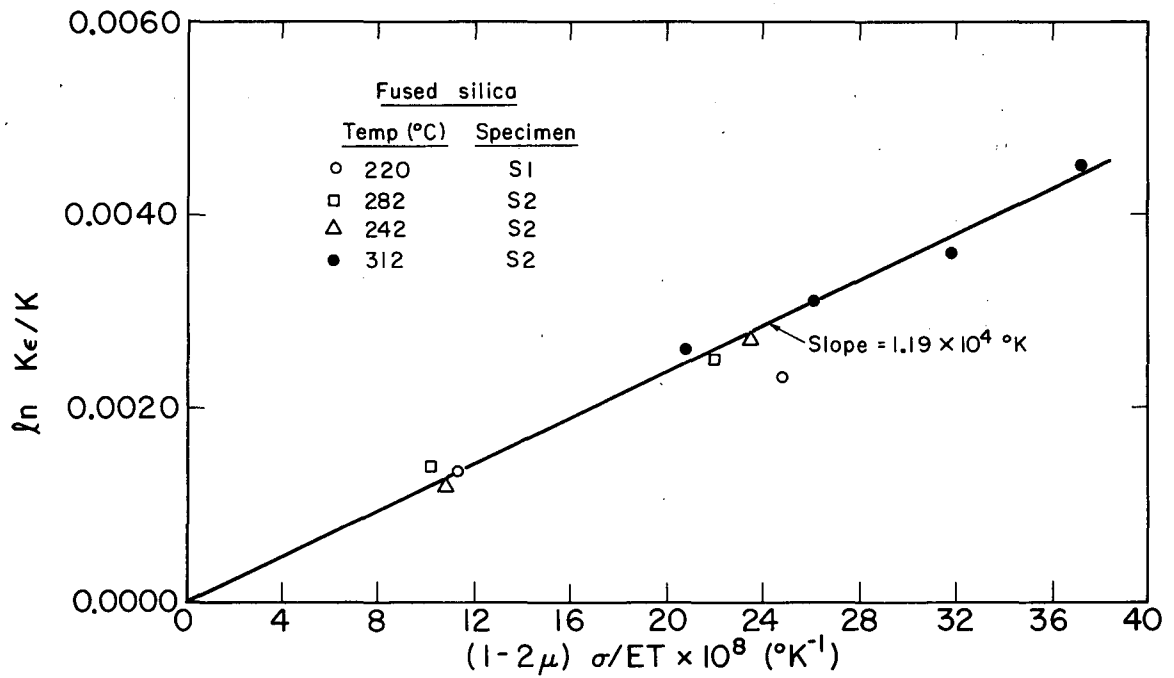
MU-30545

Fig. 17. Temperature and stress dependence of the permeability coefficient; mullite 1, unmodified specimens.



MU-30546

Fig. 18. Temperature and stress dependence of the permeability coefficient; mullite 2.



MU-30547

Fig. 19. Temperature and stress dependence of the permeability coefficient; fused silica.

There is less scatter in Fig. 19 than in Figs. 16, 17 and 18 because the absolute magnitude of the effect was two to three times larger than in the mullite specimens. Measurement of the change in permeation rate upon application of stress consequently had less error than in similar measurements for mullite. In addition, the effect of temperature gradients in the specimen were less severe since much lower temperatures were used.

The linearity of Fig. 19 shows that Eq. (15) is valid for this system. Since pure silica is a glass-former without phase boundaries, any stress effect observed must be attributed to the glassy structure. The tabulation of data is given in Table VII, Appendix D.

#### E. Loading-Rate Dependence

The rate of loading for all specimens varied between about 12 000 and 600 psi/sec. Any loading-rate dependence of permeation could not be detected within the loading-rate range employed.

#### IV. DISCUSSION

##### A. Alumina 1 and 2

The negative results of these tests indicate that the high-purity polycrystalline alumina was relatively impermeable to gases at the temperatures used. Previous reports concerning the impermeable nature of polycrystalline alumina at the test temperatures used are supported by this work.<sup>19</sup> A report of measurement of helium diffusion through alumina single crystal and polycrystalline material at 25°C and above by a similar technique is not supported.<sup>20</sup>

Stress-induced flow of helium through polycrystalline alumina, as observed by Studt,<sup>11</sup> was not detected. This may indicate sensitivity of the phenomenon to ceramic microstructure and loading rate, as suggested by Studt, who postulated that a flow of helium occurred for several hundred microns distance through interconnected pores. A small number, or complete absence, of interconnected pores in specimens of this investigation may have prevented detection of a stress-induced flow.

##### B. Measurement of K and D in Mullite 1

Experimental determination of K was felt to be more accurate than D because of design limitations of the apparatus. A given steady-state temperature could be maintained at  $\pm 2^\circ\text{C}$  with the furnace either evacuated to  $10^{-4}$  mm Hg or filled with 1 atmos helium. The difference in mass spectrometer output at the two conditions was then readily determined, and was used to calculate K.

An accurate determination of D required that the temperature of the specimen remain essentially constant when helium was evacuated from the furnace. Unless extreme care was taken in evacuation of the furnace, rapid fluctuation in the temperature of the specimen occurred.

Reproducible D values were obtained experimentally when temperature variation was minimized to  $\pm 5^\circ\text{C}$  and the data points were taken from about the first 20% of the decay curve. This technique avoided excessive contribution from changes in the rate of helium permeation

through the thick walled portion. Because of the nonideal conditions which existed, an absolute accuracy could not be assigned to the specific values of K and D reported. The values  $\Delta H_D$  and  $\Delta H_K$  have an accuracy of about  $\pm 2000$  cal/mole and  $\pm 1500$  cal/mole respectively. These ranges were determined by the maximum and minimum slopes of reasonable straight lines drawn through the data points of Figs. 12 and 13. The order of magnitude of K and D and the values of  $\Delta H_K$  and  $\Delta H_D$  within the accuracy stated are useful information.

### C. Glassy-Phase Composition of Mullite 1

Altemose has developed an empirical expression for the activation energy of permeation of helium through glass as a function of the amount of network former.<sup>12</sup> He has shown that

$$\Delta H_K = - 260 M + 30 \times 10^3 \text{ cal/mole}, \quad (18)$$

where M is the mole percent of network former.

Altemose assumed an irregular glass lattice as described by Zachariassen,<sup>21</sup> and used by Norton.<sup>22</sup> The network formers, such as  $\text{SiO}_2$ , were pictured as completing a chainlike network with openings large enough for small gas molecules to permeate. Addition of alkali oxides and alkaline earth oxides acted to plug these openings.

Studt has shown that an empirical expression similar to Eq. (18) may be written for the activation energy of diffusion of helium in glass.<sup>11</sup> Here we have

$$\Delta H_D = - 130 M + 18.6 \times 10^3 \text{ cal/g atoms}, \quad (19)$$

where M is the mole percent network former.

Essentially the same glass model was used as had been assumed by Altemose.

If diffusion of helium through a glass is the rate-determining step in a permeation process, the  $\Delta H_D$  and  $\Delta H_K$  calculated from measurements will be determined by the amount of network former in the glass. Equations (18) and (19) afford a convenient method of estimating the amount of network former in the glassy phase of complex ceramics.

Equations (18) and (19) were used with values of  $\Delta H_K$  and  $\Delta H_D$ , determined experimentally, to estimate the amount of glass former in mullite 1. The results were:

- (a) By Eq. (18),  $M = 82.5$  mole percent network former, and
- (b) by Eq. (19),  $M = 68.3$  mole percent network former. These two values differ by about 17%. However, within the experimental error given for  $\Delta H_K$  and  $\Delta H_D$ , the estimation is reasonable and agrees approximately with the chemical analysis.

#### D. Effect of Crystalline Content on Gaseous Permeation

Swets et al. have studied helium diffusion through pure fused silica in the temperature range 500 to 800°C.<sup>9</sup> They report  $K$  and  $D$  values on the order of  $10^{12} - 10^{13}$  atoms/sec cm and  $10^{-5}$  cm<sup>2</sup>/sec respectively. Altemose has reported similar values of  $K$  for helium diffusion through twenty different glass compositions.<sup>12</sup>

Values of  $K$  and  $D$  obtained in this investigation for helium diffusion through mullite 1 were on the order of  $10^{10}$  atoms/sec cm and  $10^{-6}$  cm<sup>2</sup>/sec respectively. The measured  $K$  and  $D$  values are one to three orders of magnitude smaller than they would have been if the  $K$  and  $D$  values of the pure glass phase had been measured. The qualitative effect of the reduction of  $K$  and  $D$  by the presence of relatively impermeable phases in a glassy matrix can be explained by two considerations:

First, the glassy area per unit area of material available for diffusion perpendicular to flow direction is reduced. Secondly, the length of the path a gas atom must take in diffusing through a glassy medium is increased. The microphotograph of mullite 2 (Fig. 5) is a good example of this point. It can be seen that the path taken by a gas atom through the glassy phase could be much longer than the simple perpendicular distance between two parallel planes several grain diameters apart.

In the course of these experiments, the decrease in  $K$  and  $D$  by inclusion of relatively impermeable crystalline material in a glassy matrix was observed qualitatively.

The time between introduction of helium and achievement of steady-state permeation was observed for each material. After a correction had been made for the difference in wall thickness, the elapsed time was seen to be different for each material at the same temperature. In order of increasing elapsed time to reach steady state, the materials were fused silica, mullite 1, and mullite 2. The materials giving decreasing magnitude of the steady-state helium permeation followed in the same order.

#### E. Stress Dependence of Permeation in Mullite and Fused Silica

A sudden change in  $D$  caused by step change in temperature will result in a step change in the flow rate of helium. The solubility of helium,  $S$ , also has a step change. However, the change in  $S$  is not detected immediately because a finite length of time elapses before the concentration gradient is changed on the low-pressure side. Use has been made of this phenomenon for experimental determination of  $\Delta H_D$  and  $\Delta H_S$  of helium diffusion through germanium.<sup>23</sup>

If we assume that the change in  $D$  and  $S$  by a step change in temperature is analogous to change by mechanical strain, the same phenomenon should operate. In obtaining Eq. (15), the original assumption was made that  $S$  would remain essentially constant, while  $D$  would change by strain. The validity of this assumption was shown by the experimental observation that upon application or removal of a load, the flow rate immediately changed to a new steady-state condition. No change in flow rate was detected after the initial change even after periods of twenty minutes in the stressed condition.

The maximum observed increase in helium flow rate upon stress application was about 1.4% at a stress level of 4600 psi in a modified specimen of mullite 1. Any disturbance of the helium concentration gradient on the low-pressure side in the materials, by step change in flow of this order of magnitude, was not detected.

The results of tests of fused silica supports the assumption that the effect of stress observed in mullite was probably due to strain

in the glassy phase. The stress dependence of the permeation of helium through mullite appears to be determined to a great extent by Young's modulus of the glassy phase. This is reasonable, since the slowest step in the permeation process of the diffusing specie is presumably the jumping of helium atoms between ions in the glass network.<sup>12, 19</sup> From these observations it is to be expected that, in complex ceramics containing a significant amount of glassy phase, the stress dependence of gaseous permeation will increase rapidly at higher temperatures, whereas the elasticity of the glassy phase usually decreases precipitously.

The slopes of the lines drawn through the data in Figs. 16 through 19 are equal to  $M/k$ , as shown in Eq. (15). It is interesting to note that the values of  $M/k$  obtained from these slopes have an order-of-magnitude agreement with values reported for self-diffusion in several strained metal crystals.<sup>7</sup>

The value of the parameter  $M$  has been shown to be characteristic of a given material and diffusing species.<sup>7</sup>  $M$  can be considered the strain coefficient of the activation energy of diffusion. From a physical viewpoint, the value of  $M$  is reasonably related to  $\Delta H_D$ . The fact that the slope of Fig. 19 is much less than that of Fig. 16 is possibly related to the fact that  $\Delta H_D$  of helium in fused silica is less than  $\Delta H_D$  of helium in mullite 1.

The phase boundaries of the alumina and mullite materials tested were evidently stress-bearing. A gradual accumulation of flaws introduced by cyclic tensile stresses was not detected. Failure always occurred in tension by brittle fracture, with no previous change in the permeation rate or its stress dependence.

## V. SUMMARY AND CONCLUSION

The tensile stress dependence of helium permeation through complex ceramics and fused silica was investigated.

No helium permeation was detected in tests on two high-purity alumina materials of different microstructure.

Volume diffusion through the glassy phase appeared to be the controlling step in the permeation process in the two polyphase mullite materials and fused silica.

Tensile stresses imposed on these materials resulted in increased steady-state helium permeation. The maximum increase in permeation rate observed was 1.4% at a stress level of 4600 psi. The effect was reversible and no deterioration of the materials, or change in the helium diffusion mechanism, due to cyclic or static stress application was detected.

It was concluded that the observed stress dependence of helium permeation through polyphase refractory mullite was determined by the effect of stress on the glassy phase of the microstructure.

The mechanism of the stress dependence of permeation appeared to be a change of the activation energy of diffusion resulting from a strain imposed on the glass structure.

The observed effect had a strong dependence on Young's modulus of the glassy phase. Therefore, the temperature dependence of Young's modulus is an important consideration in studies of the stress effect on permeation, particularly at high temperatures.

### ACKNOWLEDGMENTS

The author wishes to gratefully acknowledge the counsel and direction of Professor R. M. Fulrath during the course of this investigation.

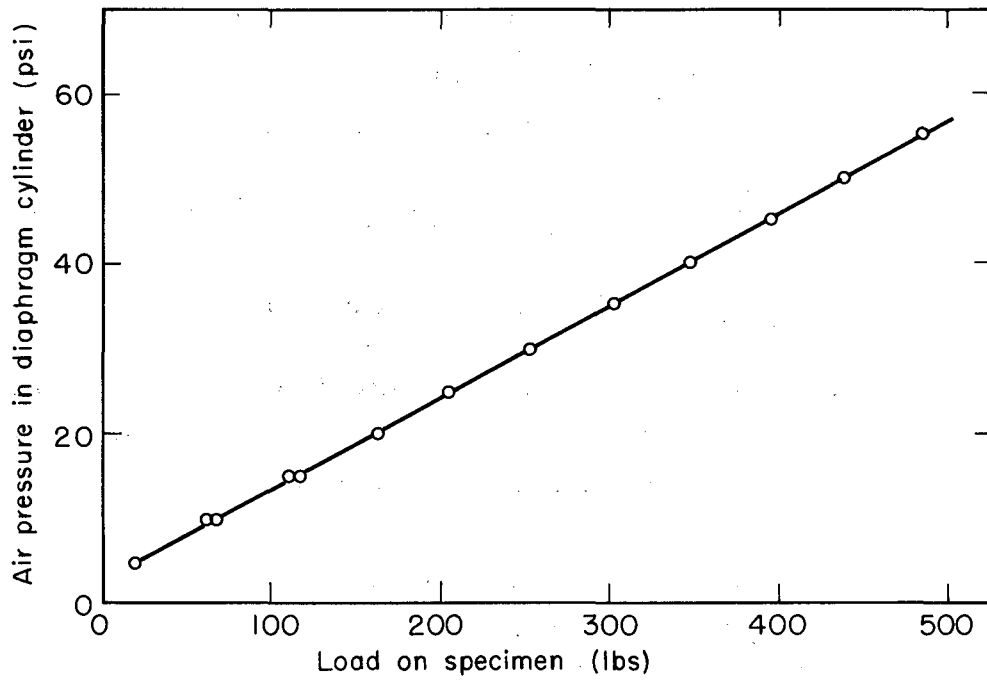
He is grateful to Mr. Larry Ernest who prepared the photomicrographs and to Mr. Stephen Firestone for general assistance.

Many helpful discussions and suggestions of Dr. Perry L. Studt and Mr. Ronald Rossi are deeply appreciated.

This work was done under the auspices of the U. S. Atomic Energy Commission.

APPENDICES

A. Calibration of the Loading Device (Diaphragm Cylinder)



MU-30548

Fig. 20. Calibration of the loading device (diaphragm cylinder).

B. Calibration of the Helium Leak Detector

Helium calibrated leak rate:  $18.6 \times 10^{-7}$  cc gas (at 1 atm, 79°F)/sec  
(temperature coefficient - 1.5%/°F)

December 26, 1962: Calibrated leak vented to the leak detector; 71°F.

Strip chart recorder reading: 84 div on  $\times 100$  scale

-background:  $\frac{-3 \text{ div}}{=81 \text{ div}}$  on  $\times 100$  scale.

Temperature correction to calibrated leak rate:

$$\begin{aligned} & [(18.6) - (79 - 71) (0.015) (18.6)] \times 10^{-7} \\ & = 16.4 \times 10^{-7} \text{ cc gas (at 1 atm, 71°F)/sec.} \end{aligned}$$

Helium leak detector sensitivity (s):

$$\begin{aligned} s &= \frac{16.4 \times 10^{-7} \text{ cc gas (at 1 atm, 71°F)}}{81 \times 100 \text{ div-sec}} \\ &= 2.02 \times 10^{-10} \frac{\text{cc gas (at 1 atm, 71°F)}}{\text{sec-div}} \end{aligned}$$

Sensitivity can be expressed in units (atoms/sec-div) by the following calculations. Sensitivity in these units is designated (s'):

From the ideal gas law,  $PV = nRT$ ,

where

n = number of moles of gas,

p = pressure (atmos),

V = volume (cc),

R = gas constant (82.06 cc-atmos/deg-mole),

T = absolute temperature (71°C = 295°K).

Sensitivity can be written as

$$s = PV/\text{sec-div} = nRT/(\text{sec-div}) = 2.02 \times 10^{-10} \text{ cc atm/sec-div.}$$

Now  $s' = sN/RT = n/\text{sec-div}$ , where N is Avogadro's number,

$$\text{and } s' = \frac{(2.02 \times 10^{-10} \text{ cc-atmos/sec-div}) (6.023 \times 10^{23} \text{ atoms/mole})}{(82.06 \text{ cc-atm/deg-mole}) (295^\circ \text{K})}$$

$$= 5.21 \times 10^9 \text{ atoms/sec-div.}$$

C. Mathematics of the Method of Determination of Diffusion and Permeation Coefficients

The assumption was made that, in all measurements, permeation of the gas through the wall was determined only by the bulk diffusion process, this being the slowest of the successive processes which make up the whole permeation process.

The permeation  $F$  through the cylindrical surface of the specimen is measured in atoms per second and is a function of the diffusion coefficient and the concentration gradient at  $r = a$ , (see Fig. 21).

The permeation measured is:

$$F = - AD \left( \frac{dc}{dr} \right)_{r=a} \text{ atoms/sec,} \quad (20)$$

where

$A$  = inside area of the cylinder ( $\text{cm}^2$ ),

$D$  = diffusion coefficient ( $\text{cm}^2/\text{sec}$ ),

$(dc/dr)_{r=a}$  = concentration gradient (in atoms/ $\text{cm}^3$ -cm at  $r = a$ ).

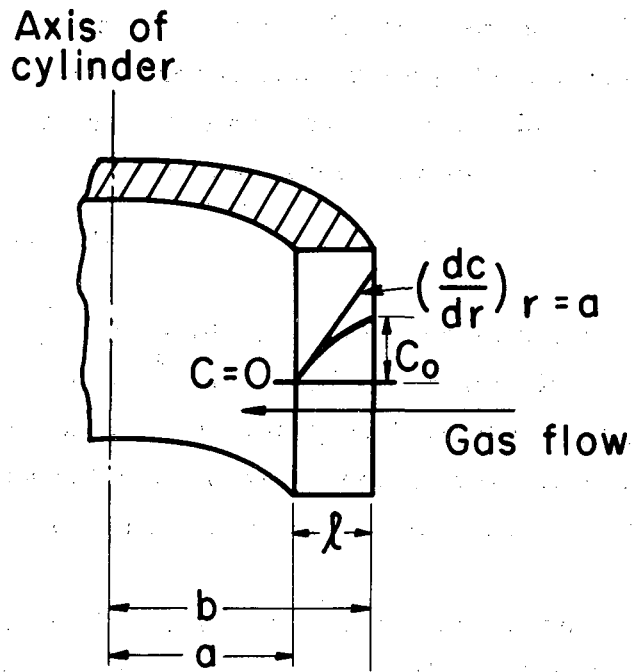
The inside of the cylinder is exposed to the vacuum of the mass spectrometer and the outside either to a vacuum ( $10^{-4}$  mm Hg) or 1 atmosphere of helium.

To obtain the concentration gradient at  $r = a$ , we require a solution of Fick's diffusion equation for the hollow cylinder with the following conditions:

- (a) at  $r = a$ ,  $c = 0$  for all times  $t$ ,
- (b) at  $r = b$ ,  $c = c_0$  for all times  $t$ ,
- (c) at  $a < r < b$ ,  $c = 0$  for time  $t = 0$ .

The solution, of the form  $c = f(t, r)$  with  $D$  and  $c_0$  as parameters, is given by Carslaw and Jaeger.<sup>24</sup> Their solution is in terms of  $k = b/a$  and  $\ell = b-a$ , and from this solution the following expression can be derived:

$$\left( \frac{dc}{dr} \right)_{r=a} = \frac{c_0}{\ell} \cdot \frac{k-\ell}{\ell nk} \left\{ 1 + \frac{2k^{1/2} \ell n k}{k-1} \sum_{n=1}^{\infty} (-1)^n \exp \left[ \frac{-\pi^2 n^2}{\ell^2} Dt \right] \right\}. \quad (21)$$



MU-30549

Fig. 21. Concentration pattern during steady-state permeation in a cylindrical wall (from Ref. 23).

This expression is a good approximation for  $k$  values between 1 and approx 1.5. Values of  $k$  exceeding 1.5 involve the use of exact expressions, with Bessel functions as given in Carslaw and Jaeger.

For values of  $k$  smaller than about 1.5, the factor  $k^{1/2} I_{nk}/(k-1)$  deviates less than one percent from unity and is negligible. The factors between the brackets in Eq. (21) can be approximated by

$$1 + 2 \sum_{n=1}^{\infty} (-1)^n \exp - \left[ \frac{\pi^2 n^2}{l^2} \right] Dt . \quad (22)$$

If we let

$$q = \exp - \left[ \frac{\pi^2}{l^2} \right] Dt, \quad (23)$$

the infinite series reduces to

$$1 - 2q + 2q^4 - 2q^9 + 2q^{16} - \dots \quad (24)$$

which rapidly converges for large values of  $t$ .

For  $t = \infty$  the permeation is  $F_s$ , that of the steady state, and according to Eqs. (20) and (21) it is given by:

$$F_s = - \frac{c_0}{l} \cdot \frac{k-1}{\ln k} DA , \quad (25)$$

where  $c_0$  is the concentration of helium at  $r = b$ , and  $A$  is the inside surface area. From Eqs. (20), (21), and (25) we conclude that

$$\frac{F}{F_s} = \frac{- \left[ \frac{c_0}{l} \cdot \frac{k-1}{\ln k} (1 - 2q + 2q^4 - 2q^9 + 2q^{16} - \dots) \right] DA}{- \frac{c_0}{l} \frac{k-1}{\ln k} DA} , \quad (26)$$

and that

$$\frac{F}{F_s} = 1 - 2q + 2q^4 - 2q^9 + 2q^{16} - \dots \quad (27)$$

which holds for both directions of flow through the wall.

The permeation  $F$  is related to the mass spectrometer (leak detector) reading by:

$$F = (h) (s'), \quad (28)$$

where

$h$  = mass spectrometer reading (chart scale div)

and

$s'$  = sensitivity of mass spectrometer (atoms/sec-div).

Therefore, from Eqs. (27) and (28),

$$h = \frac{F_s}{s'l} [ 1 - 2q + 2q^4 - 2q^9 + 2q^{16} - \dots ] , \quad (29)$$

which from Eq. (25) can be written:

$$h = \frac{A D c_0}{s'l} \left[ \frac{k-1}{\ell n k} \right] [ 1 - 2q + 2q^4 - 2q^9 + 2q^{16} - \dots ] . \quad (30)$$

This equation is applicable only if the time constant for the pump-out rate of the ion source of the mass spectrometer is much smaller than the time constant for the transient effect of the diffusion process.

At steady state, the exponentials of Eq. (30) drop out, and the equation becomes

$$h_0 = \left[ \frac{A D c_0}{s'l} \right] \frac{k-1}{\ell n k} , \quad (31)$$

where

$h_0$  = the steady state reading of the mass spectrometer.

If, after steady state has been reached, the gas is suddenly removed from the outside surface of the specimen, the mass spectrometer reading will drop off as

$$h = h_0 \left\{ 2 \sum_{n=1}^{\infty} (-1)^n \exp [ -(\pi^2 n^2 / \ell^2) Dt ] \right\} , \quad (32)$$

where  $q$  has been replaced by  $\exp - [ \pi^2 / \ell^2 ] Dt$  (see Fig. 22). After a short time the mass spectrometer recorder trace becomes a simple exponential decay curve with a time constant equal to

$$t_0 = \frac{t_2 - t_1}{\ell n(h_1/h_2)} = \ell^2 / \pi^2 D , \quad (33)$$

where

$t_0$  = time constant of the decay curve (sec),

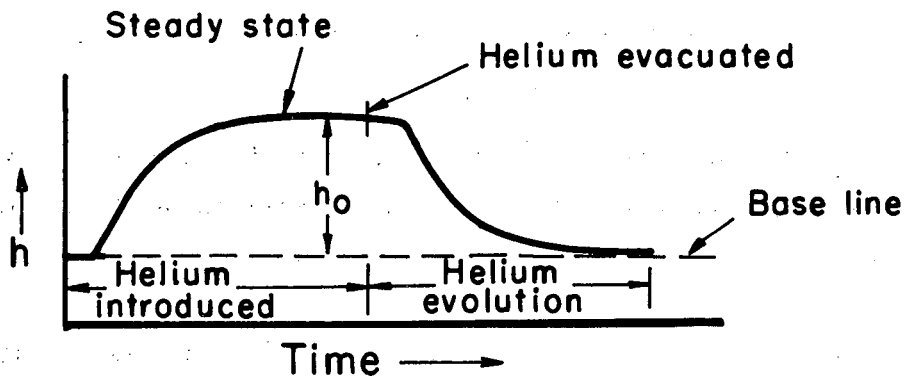
$t_1, t_2$  = time elapsed since evacuation of helium (sec),

$h_1$  = height of recorder trace at time  $t_1$  (div),

and

$h_2$  = height of recorder trace at time  $t_2$  (div) .

If the log of  $h$  is plotted vs  $t$ , a straight line will be obtained, and  $(t_0)$  is then calculated from the slope of the line. The thickness



MU-30550

Fig. 22. Typical mass spectrometer record.

of the specimen  $l$  can be measured directly with a micrometer from fragments of the test section after the experiment. Therefore,  $D$  can easily be calculated from Eq. (33).

The permeation coefficient  $K$  is obtained from the steady state mass spectrometer reading  $h_0$ , which is multiplied by

$$s'l \cdot \left\{ A \left[ \frac{k-1}{\ln k} \right] \right\}^{-1}$$

to give  $K$  in the commonly used units of atoms/cm-sec., as

$$K = h_0 \left\{ s'l \cdot \left[ A \left( \frac{k-1}{\ln k} \right) \right]^{-1} \right\}. \quad (34)$$

The factor  $A(k-1)/\ln k$  is the effective area.

As can be seen from Eq. (31),

$$K = Dc_0. \quad (35)$$

When the gas pressure outside the specimen is 1 atmos the concentration  $c_0$  inside the surface is considered to be the solubility  $S$ , therefore:

$$K = DS. \quad (36)$$

After the diffusion and permeation coefficients have been measured, the solubility can be calculated from Eq. (36).

D. Experimental Data

Table IVA. Experimental data from tests on alumina 1 and 2

Alumina sample No.	Specimen	Temp. (°C)	Minimum stress (psi)	Maximum tensile stress (psi)	Number of cycles	Cyclic load time (min)		Remarks	
						on	off		
1	M1	25	0	2000	10	1	1	No helium permeation detected.	
			0	4000	5	1	1		
		271	0	0	0	0	0	46 hr	Tests discontinued; "O" rings started to soften at higher temp. Loading device unable to fracture specimen.
			0	4500	4	1	1		
			0	5000	4	1	1		
			0	6800	10	1	1		
0	7700	10							
2	AV1B	963	0	0	0	0	18 hr	No helium permeation detected. Tests discontinued due to failure of epoxy bond between copper collar and specimen.	
			0	3500	6	1	1		
			0	5000	6	1	1		
			0	7000	6	1	1		
			0	9000	15	1	1		
			0	9000	1	30	0		

Table IVB. Experimental data from tests on alumina 2

Alumina sample No.	Specimen	Temp. (°C)	Minimum stress (psi)	Maximum tensile stress (psi)	Number of cycles	Cyclic load time (min)		Remarks
						on	off	
2	AV6B	714	0	0	0	0	14 hr	No helium permeation detected.
			0	6400	10	1	1	
			0	7400	6	1	1	
			0	8400	10	1	1	
			0	9400	5	1	1	
			0	10400	12	1	1	
2	AV6B	825	0	0	0	0	15 hr	Specimen failed at the fillet of test section upon 12th application of 12000 psi stress.
			0	7400	2	1	1	
			0	8400	4	1	1	
			0	11200	5	1	1	
			0	12000	3	1	1	
			0	12000	8	2	2	



Table VB. Tabulation of data in chronological order for mullite 1 (no test section ground on tube).<sup>a</sup>

Temp. (°C)	Unstressed flow rate $h_0$ (division)	Cyclic tensile strength $\sigma_{max}$ (psi)	Av change flow rate $\Delta h$ (division)	Number of cycles	Young's modulus ( $E \times 10^{-6}$ psi)	$\frac{(1-2\nu)\sigma}{ET} \times 10^8$ (°K <sup>-1</sup> )	$\ln K_\epsilon / K$ $\times 10^4$
746	25750	2030	57.5	10	8.48	11.72	22
746	25750	3300	120.0	13	8.48	19.12	47
746	25750	4820	154.0	14	8.48	27.90	60
866	38700	1600	15.6	14	4.00	17.60	40
866	38700	2350	20.7	15	4.00	25.90	54
866	38700	2980	28.5	12	4.00	37.20	74
553	9850	1600	22.4	12	8.70	11.10	23
553	9850	2350	28.4	11	8.70	16.25	29
553	9850	2980	37.0	15	8.70	20.60	38

<sup>a</sup>Specimen MT7 used for all data in this table.

Table VI. Tabulation of data in chronological order for mullite 2

Specimen	Temp. (°C)	Unstressed flow rate $h_0$ (divisions)	Cyclic tensile stress $\sigma_{max}$ (psi)	Av change flow rate $\Delta h$ (divisions)	Number of cycles	Young's modulus $E \times 10^{-6}$ (psi)	$\frac{(1-2\nu)\sigma}{ET}$ $\times 10^8$ (°K <sup>-1</sup> )	$\ln \left( \frac{K_c}{K} \right)$	
MM3 <sup>a</sup>	716	5 770	2620	20	13	8.56	15.5	0.0035	
			3100	25	14		18.1	0.0043	
MM4 <sup>a</sup>	919	18 560	1650	65	8	3.75	18.4	0.0035	
			2140	126	10		23.8	0.0068	
			2600	132	12		29.0	0.0071	
			3090	139	13		34.5	0.0075	
	939			1650		14	3.20	21.2	0.0030
				2140		12		27.5	0.0036
				2600		12		33.4	0.0043
				3090		12		39.8	0.0055
	820			1650		12		9.4	0.0034
				2140		12		12.2	0.0038
				2600		13		14.9	0.0038
				3090		12		17.6	0.0051
	756			2600		13	8.46	14.9	0.0027
3090					13	17.8		0.0036	
3580					13	20.6		0.0042	
4070					12	23.4		0.0041	
685			1650		13	8.61	9.9	0.0036	
			3560		21		21.6	0.0068	

<sup>a</sup>No test section ground on tube.

Table VII. Tabulation of data in chronological order for fused silica

Specimen	Temp. (°C)	Unstressed flowrate $h_0$ (divisions)	Cyclic tensile stress $\sigma_{max}$ (psi)	Av change flowrate $\Delta h$ (divisions)	Number of cycles	Young's modulus $E \times 10^{-6}$ (psi)	$\frac{(1-2\nu)\sigma}{ET} \times 10^8$ (°K <sup>-1</sup> )	$\ln \left( \frac{K \epsilon}{K} \right)$
S1 <sup>a</sup>	220	31 000	850	42	13	10.8	11.3	0.00135
		31 000	1840	72	15		24.8	0.00232
S2 <sup>a</sup>	282	50 000	850	70.7	16	10.8	10.1	0.0014
			1840	127.0	15		22.0	0.0025
	242	38 500	850	44.7	17		10.9	0.0012
			1840	103.0	15	10.8	23.5	0.0027
	312	64 000	1840	166	15	10.8	20.8	0.0026
			2320	199	15		26.1	0.0031
			2830	229	11		31.8	0.0036
3330			286	11		37.2	0.0045	
		3800	364	12		42.8	0.0057	

<sup>a</sup>No test section ground on tube.

REFERENCES

1. J. P. Roberts, Gastightness of Ceramics, in Transactions of the Seventh International Ceramic Congress, London (1960).
2. G. J. Dienes, G. H. Vineyard, Radiation Effects in Solids(Inter-science Publishers, Inc., New York, 1957), p. 39.
3. R. M. Barrer, Diffusion in and Through Solids, (Cambridge University Press London, 1941).
4. W. Jost, Diffusion in Solids, Liquids, Gases, (Academic Press, Inc., New York, 1952).
5. P. C. Carman, Flow of Gases through Porous Media, (Academic Press Inc., New York, 1956), pp. 1,67,131.
6. T. Liu, and H. G. Drickamer, The Effect of Compression and of Hydrostatic Pressure on Diffusion Anisotropy in Zinc, *J. Chem. Phys.* 22, 312 (1954).
7. L. A. Girifalco and H. H. Grimes, Effect of Static Strains on Diffusion, *Phys. Rev.* 121, 982 (1961).
8. E. W. Sucov, Diffusion of Oxygen in Vitreous Silica, *J. Am. Ceram. Soc.* 46, 14 (1963).
9. D. E. Swets, R. W. Lee and R. C. Frank, Diffusion Coefficients of Helium in Fused Quartz, *J. Chem. Phys.* 34, 17 (1961).
10. K. B. McAfee, Jr., Stress-Enhanced Diffusion in Glass: I. Glass Under Tension and Compression, "*J. Chem. Phys.* 28, 218 (1958).
11. P. L. Studt, Mechanism of Gaseous Permeation Through Glass, Single-Crystal Silicon, and Germanium; and Stress-Enhanced Gaseous Permeation Through Alumina Bodies (Ph. D. Thesis), Lawrence Radiation Laboratory Report UCRL-10466, September 26, 1962 (unpublished).
12. V. O. Altemose, Helium Diffusion Through Glass, *J. Appl. Phys.* 32, 1309 (1961).
13. W. D. Kingery, Introduction to Ceramics (John Wiley and Sons, Inc., New York, 1960), p. 243.

14. J. B. Wachtman, Jr. and D. G. Lam, Jr., Young's Modulus of Various Refractory Materials as a Function of Temperature, *J. Am. Ceram. Soc.* 42, 254 (1959).
15. G. K. Dunsmore, J. E. Fenstermacher, and F. A. Hummel, High Temperature Mechanical Properties of Ceramics Materials: III. Vitrified Chemical and Refractory Porcelains, *Bull. Am. Ceram. Soc.* 40, 310 (1961).
16. S. Spinner, Elastic Moduli of Glasses at Elevated Temperature by a Dynamic Method, *J. Am. Ceram. Soc.* 39, 113 (1956).
17. J. W. Marx and J. M. Sivertsen, Temperature Dependence of the Elastic Moduli and Internal Friction of Silica and Glass, *J. Appl. Phys.* 24, 81 (1953).
18. S. Spinner, Temperature Dependence of Elastic Constants of Vitreous Silica, *J. Am. Ceram. Soc.* 45, 394 (1962).
19. D. Hayes, D. W. Budworth and J. P. Roberts, Selective Permeation of Gases Through Dense Sintered Alumina, *Trans. Brit. Ceram. Soc.* 60, 494 (1961).
20. W. B. Campbell, Diffusion Rate and Activation Energy of Helium Through Single-Crystal and Polycrystal Alumina, (M. S. Thesis), Georgia Institute of Technology, 1960.
21. W. H. Zachariasen, The Atomic Arrangement in Glass, *J. Am. Chem. Soc.* 54, 3841 (1932).
22. F. J. Norton, Helium Diffusion Through Glass, *J. Am. Ceram. Soc.* 36, 90 (1953).
23. A. Van Wieringen and N. Warmoltz, On the Permeation of Hydrogen and Helium in Single-Crystal Silicon and Germanium at Elevated Temperatures, *Physica* 22, 849 (1956).
24. H. S. Carslaw and J. C. Jaeger, Conduction of Heat in Solids (Clarendon Press, Oxford, 1947), p. 178.

This report was prepared as an account of Government sponsored work. Neither the United States, nor the Commission, nor any person acting on behalf of the Commission:

- A. Makes any warranty or representation, expressed or implied, with respect to the accuracy, completeness, or usefulness of the information contained in this report, or that the use of any information, apparatus, method, or process disclosed in this report may not infringe privately owned rights; or
- B. Assumes any liabilities with respect to the use of, or for damages resulting from the use of any information, apparatus, method, or process disclosed in this report.

As used in the above, "person acting on behalf of the Commission" includes any employee or contractor of the Commission, or employee of such contractor, to the extent that such employee or contractor of the Commission, or employee of such contractor prepares, disseminates, or provides access to, any information pursuant to his employment or contract with the Commission, or his employment with such contractor.

Faint, illegible text covering the majority of the page, possibly representing a list or a set of instructions.

